Defense Threat Reduction Agency
8725 John J. Kingman Road, MS
6201 Fort Belvoir, VA 22060-6201

DTRA-TR-16-62

TECHNICAL REPORT

Novel Protection and Decontamination Strategies

June 2016

HDTRA1-09-1-0004

Sharon Isern et al.

Prepared by:
Florida Gulf Coast Univ.
10501 Gulf Coast Blvd. South
Fort Myers, FL 33965

DESTRUCTION NOTICE:

Destroy this report when it is no longer needed.
Do not return to sender.

PLEASE NOTIFY THE DEFENSE THREAT REDUCTION AGENCY, ATTN: DTRIAC/ J9STT, 8725 JOHN J. KINGMAN ROAD, MS-6201, FT BELVOIR, VA 22060-6201, IF YOUR ADDRESS IS INCORRECT, IF YOU WISH IT DELETED FROM THE DISTRIBUTION LIST, OR IF THE ADDRESSEE IS NO LONGER EMPLOYED BY YOUR ORGANIZATION.

REPORT DOCUMENTATION PAGE

Form Approved
OMB No. 0704-0188

1. REPORT DATE *(DD-MM-YYYY)*	2. REPORT TYPE	3. DATES COVERED *(From - To)*
06-29-2011	Final Technical Report	04-05-2009 - 04-04-11

4. TITLE AND SUBTITLE
Novel Protection and Decontamination Strategies

5a. CONTRACT NUMBER

5b. GRANT NUMBER
HDTRA1-09-1-0004

5c. PROGRAM ELEMENT NUMBER

6. AUTHOR(S)
Isern, Sharon (PI)
Barreto, Jose, C (co-PI)
Michael, Scott, F (co-PI)

5d. PROJECT NUMBER

5e. TASK NUMBER

5f. WORK UNIT NUMBER

7. PERFORMING ORGANIZATION NAME(S) AND ADDRESS(ES)
Florida Gulf Coast University
10501 FGCU Blvd. South
Fort Myers, FL 33965-6565

8. PERFORMING ORGANIZATION REPORT NUMBER

9. SPONSORING/MONITORING AGENCY NAME(S) AND ADDRESS(ES)
DTRA/BE-BCR
8725 John J. Kingman Road
MSC 6201
Fort Belvoir, VA 22060-6201

10. SPONSOR/MONITOR'S ACRONYM(S)

11. SPONSOR/MONITOR'S REPORT NUMBER(S)

12. DISTRIBUTION/AVAILABILITY STATEMENT

13. SUPPLEMENTARY NOTES

14. ABSTRACT

The basic premise of this work was to conduct basic science investigations into novel technologies to protect against and decontaminate biological agents and toxins that can be applied to both civilian and military use. The work can be divided into investigations into two broad topic areas: development of novel rationally designed virus inactivation strategies and novel environmentally benign disinfection systems. The virus inactivation work during this project led to: (1) The discovery and characterization of multiple distinct peptide inhibitors of dengue virus infectivity, including novel chemically modified peptide inhibitors with improved pharmacological properties. (2) The first description and characterization of the human humoral immune response against dengue virus in the form of human monoclonal antibodies against the virus surface envelope protein. Many of these antibodies show neutralizing activity against dengue virus and can form the basis of prophylactic or therapeutic treatments. The decontamination work during this project led to: (3) Invention and final patent application for a family of new 'switchable' germicides with sub-contractor testing showing excellent efficacy against bacterial pathogens. (4) The discovery that a combination of bromide and ferric ions greatly enhanced photocatalytic destruction of a lipid target, with a bromide mediated mechanism, creating products similar to those observed during gamma ray decontamination.

15. SUBJECT TERMS
virus, dengue, inhibitor, peptide, human monoclonal antibody, photocatalysis, germicides, decontamination, alkaline biocides

16. SECURITY CLASSIFICATION OF:			17. LIMITATION OF ABSTRACT	18. NUMBER OF PAGES	19a. NAME OF RESPONSIBLE PERSON
a. REPORT	b. ABSTRACT	c. THIS PAGE			Sharon Isern, Ph.D.
U	U	U	UU	47	19b. TELEPHONE NUMBER *(Include area code)* 239-590-7438

Reset

Standard Form 298 (Rev. 8/98)
Prescribed by ANSI Std. Z39.18

UNIT CONVERSION TABLE

U.S. customary units to and from international units of measurement*

U.S. Customary Units	Multiply by → / ← Divide by†		International Units
Length/Area/Volume			
inch (in)	2.54	$\times 10^{-2}$	meter (m)
foot (ft)	3.048	$\times 10^{-1}$	meter (m)
yard (yd)	9.144	$\times 10^{-1}$	meter (m)
mile (mi, international)	1.609 344	$\times 10^{3}$	meter (m)
mile (nmi, nautical, U.S.)	1.852	$\times 10^{3}$	meter (m)
barn (b)	1	$\times 10^{-28}$	square meter (m^2)
gallon (gal, U.S. liquid)	3.785 412	$\times 10^{-3}$	cubic meter (m^3)
cubic foot (ft^3)	2.831 685	$\times 10^{-2}$	cubic meter (m^3)
Mass/Density			
pound (lb)	4.535 924	$\times 10^{-1}$	kilogram (kg)
unified atomic mass unit (amu)	1.660 539	$\times 10^{-27}$	kilogram (kg)
pound-mass per cubic foot (lb ft^{-3})	1.601 846	$\times 10^{1}$	kilogram per cubic meter (kg m^{-3})
pound-force (lbf avoirdupois)	4.448 222		newton (N)
Energy/Work/Power			
electron volt (eV)	1.602 177	$\times 10^{-19}$	joule (J)
erg	1	$\times 10^{-7}$	joule (J)
kiloton (kt) (TNT equivalent)	4.184	$\times 10^{12}$	joule (J)
British thermal unit (Btu) (thermochemical)	1.054 350	$\times 10^{3}$	joule (J)
foot-pound-force (ft lbf)	1.355 818		joule (J)
calorie (cal) (thermochemical)	4.184		joule (J)
Pressure			
atmosphere (atm)	1.013 250	$\times 10^{5}$	pascal (Pa)
pound force per square inch (psi)	6.984 757	$\times 10^{3}$	pascal (Pa)
Temperature			
degree Fahrenheit (^oF)	$[T(^oF) - 32]/1.8$		degree Celsius (^oC)
degree Fahrenheit (^oF)	$[T(^oF) + 459.67]/1.8$		kelvin (K)
Radiation			
curie (Ci) [activity of radionuclides]	3.7	$\times 10^{10}$	per second (s^{-1}) [becquerel (Bq)]
roentgen (R) [air exposure]	2.579 760	$\times 10^{-4}$	coulomb per kilogram (C kg^{-1})
rad [absorbed dose]	1	$\times 10^{-2}$	joule per kilogram (J kg^{-1}) [gray (Gy)]
rem [equivalent and effective dose]	1	$\times 10^{-2}$	joule per kilogram (J kg^{-1}) [sievert (Sv)]

*Specific details regarding the implementation of SI units may be viewed at http://www.bipm.org/en/si/.

†Multiply the U.S. customary unit by the factor to get the international unit. Divide the international unit by the factor to get the U.S. customary unit.

Abstract

The basic premise of this work was to conduct basic science investigations into novel technologies to protect against and decontaminate biological agents and toxins that can be applied to both civilian and military use. The work can be divided into investigations into two broad topic areas: development of novel rationally designed virus inactivation strategies and novel environmentally benign disinfection systems. The virus inactivation work during this project led to: (1) The discovery and characterization of multiple distinct peptide inhibitors of dengue virus infectivity, including novel chemically modified peptide inhibitors with improved pharmacological properties. (2) The first description and characterization of the human humoral immune response against dengue virus in the form of human monoclonal antibodies against the virus surface envelope protein. Many of these antibodies show neutralizing activity against dengue virus and can form the basis of prophylactic or therapeutic treatments. The decontamination work during this project led to: (3) Invention and final patent application for a family of new 'switchable' germicides with sub-contractor testing showing excellent efficacy against bacterial pathogens. (4) The discovery that a combination of bromide and ferric ions greatly enhanced photocatalytic destruction of a lipid target, with a bromide mediated mechanism, creating products similar to those observed during gamma ray decontamination.

Table of Contents

List of Figures

List of Tables

Executive Summary

The specific aims of this work can be divided into investigations into two broad, basic science topic areas: development of novel rationally designed virus inactivation strategies and novel environmentally benign disinfection systems. Our investigations related to virus inactivation have led to the discovery, characterization, and optimization of inhibitory peptides that target to distinct portions of the dengue virus surface envelope protein. These inhibitors have different properties and distinct mechanisms of action. We have modified one such peptide into the first ever "retro-inverso" antiviral peptide. Consisting of a reversed amino acid sequence and all non-natural "inverted chirality" D-amino acids, this peptide retains virus inhibitory activity, but is expected to be metabolically inert. This means that, unlike natural peptide drugs, this peptide will be resistant to degradation in the body and will have a longer pharmacological half life and may even be able to function when administered orally. Anticipating that the development of resistance to any antiviral drug will be a major concern, we have conducted selection experiments against our inhibitors and shown phenotypic evidence for the development of resistance. Our investigations into the human humoral immune response to dengue have led to the first ever description of human monoclonal antibodies against the viral surface proteins. Prior to our work, all previously published investigations had focused on the mouse immune response, which we have shown is different from the human response. We have identified and characterized multiple different human monoclonal antibodies and shown that some enhance dengue infection under certain conditions, while other neutralize infection. Understanding how enhancing versus neutralizing antibodies are produced during natural infections will directly inform the design of safer vaccine strategies against this major pathogen. Combinations of neutralizing monoclonal antibodies are likely to be useful as a therapeutic approach to this disease.

Our basic science investigations related to environmentally benign disinfection systems led to 'proof of principle' and final patent application for a family of new 'switchable' germicides (Barreto, 2011). We invented these germicides by initially screening for lethality with membrane models. We showed that alcohols, detergents and a high external pH gradient produced a large inward flux of base that elevated the pH of the internal compartment. We used luminescent, non-pathogenic, *Vibrio fischeri* to screen various alkaline germicide formulas for lethality. Abolition of bacterial luminescence allowed us to determine complete killing. We confirmed that the abolition of luminescence constituted killing by measuring turbidity, which is caused by growing numbers of bacteria and also failed to appear upon germicidal treatment. Final testing of the germicides proceeded with an independent sub-contractor lab and involved bacterial pathogens. These pathogens were monitored for killing with turbidity and colony counts on agar plates. Most of the formulas were very efficacious. We selected one formulation that killed every pathogen in our tests, and we report that data in detail herein.

Destruction of lipid targets in the plasma membrane of living cells leads to cell death so we used a lipophilic model toxin target (Sudan red IV) ensconced in the hydrocarbon core of a CTAB detergent micelle, we had previously reported that such a sequestered target poses great challenges with regard to destruction (Coates & Barreto et al., 2007) although, in a related project we showed destruction of sudan red in an ambient air environment when deposited on the surface of a photocatalyst (Finn & Barreto et al., 2011). Sudan red is inert to UV destruction and is difficult to destroy photocatalytically, in the absence of enhancing components. Very effective destructive enhancements were discovered and tested, which involved the addition of bromide

anions and ferric ions. Br_3^- production from sodium bromide has been reported in the gamma irradiation literature (Balcerzyk et al., 2011) so we designed experiments to produce Br_3^- photocatalytically. In the presence of bromide, the destructive mechanism appears to involve Br radicals and oxidants and resembles gamma ray destructive activity. We were able to demonstrate production of Br_3^- from sodium bromide solutions using TiO_2 photocatalysis and are adapting this reaction as a photocatalytic dosimeter (the same dosimetric application has been proposed by radiation scientists. The similarity in outcome to gamma radiation is important, because TiO_2 photocatalytic decontamination can be performed using the same illumination intensity as ambient sunlight, but, with much greater safety and convenience when compared to gamma ray decontamination. Our 'enhanced' bromide/ferric ion enhanced photocatalytic system rapidly leads to molecular destruction of a sequestered lipophilic target. Such a system has great potential for decontamination of toxins and for future studies of germicidal activity.

In alphabetical order, following are the personnel that were involved in the research effort: Holly Aberle – undergraduate student, Kelli Barr, Ph.D. – postdoctoral fellow, Jose Barreto, Ph.D. – co-PI, faculty, Patricia Barreto – research associate, Jordan Brown – undergraduate student, Joshua Costin, Ph.D. – postdoctoral fellow, Steven Cullipher – graduate student, Ludovic JJ Donaghy, PhD. – postdoctoral fellow, Marielys Figueroa Sierra – undergraduate student, Shane Finn – undergraduate student, Amanda Graham – technician, Andrew Griffith – technician, Shaun Gutstein – undergraduate student, Megan Herscher – undergraduate student, Mary Hodges – undergraduate student, Maria Irriano-Renno – undergraduate student, Sharon Isern, Ph.D. – PI, faculty, April Jordan – technician, Joseph Lepo, Ph.D. – University of West Florida subcontractor, faculty, Scott Michael, Ph.D. – co-PI, faculty, Cindo Nicholson – technician, Christoph Radtke – undergraduate student, Dawne Rowe – technician, Aswani Volety, Ph.D. – faculty, Scott Wessels – undergraduate student, and Carmeline Williams – technician.

The following peer-reviewed publications stemmed from the research effort:

Costin JM, Jenwitheesuk E, Lok S-M, Hunsperger E, Conrads KA, Fontaine KA, Rees CR, Rossmann MG, Isern S, Samudrala R, Michael SF. "Structural optimization and de novo design of dengue virus entry inhibitory peptides". *PLoS Neglected Tropical Diseases* 4(6): e721 doi: 10.1371/journal.pntd.0000721 (2010).

Finn ST, Strnad JA, Barreto PD, Fox ME, Torres J, Sweeney JD, Barreto JC. "A screening technique useful for testing the effectiveness of novel 'self-cleaning' photocatalytic surfaces". *Photochemistry and Photobiology* in press (2011).

Nicholson CO, Costin JM, Rowe DK, Lin L, Jenwitheesuk E, Samudrala R, Isern S, Michael SF. "Viral entry inhibitors block dengue antibody-dependent enhancement in vitro", *Antiviral Research* 2011 89:71–74 (2011).

Schieffelin JS, Costin JM, Nicholson CO, Orgeron NM, Fontaine KA, Isern, S, Michael SF, Robinson JE. "Neutralizing and non-neutralizing monoclonal antibodies against dengue virus E protein derived from a naturally infected patient". *Virology Journal* 7:28 (2010).

A thesis "Determination of the importance of three reactive oxygen species in a novel photocatalytic system used to oxidize model organic toxicants" resulted from this work

(Cullipher, Steven Thesis (M.S.) Florida Gulf Coast University 2010). The most significant conclusions of this work are: (1) an anodized titanium foil photocatalyst can destroy Sudan red, a hydrophobic micelle encapsulated dye, and (2) superoxide and hydrogen peroxide production appear to play a minor role in dye destruction.

Specific Aims

Task 1: Peptide inhibitor optimization

Introduction

We proposed originally to computationally design peptides with anti-viral activity against dengue virus using a residue-specific all-atom probability discriminatory function (RAPDF) scoring approach (Huang et al., 2000; Samudrala et al., 1998). We also proposed to use phage display technology to screen peptide mutant libraries and select for enhanced binding peptide variants, and to chemically modify the resulting peptides for increased activity and pharmacological properties. We have made excellent progress on these proposed activities and have published two peer-reviewed papers describing our results.

The available x-ray crystallography structures of dengue virus E protein were used as templates. For each peptide, we selected residues from the target region. The side chains of these peptide residues were then substituted with alternate side chains, based on a linear repulsive steric energy term provided by SCWRL version 3.0. The resulting all-atom model was energy minimized using the Energy Calculation and Dynamics (ENCAD) program. The RAPDF score was then applied to the energy minimized peptides to estimate the structural stability. The peptides that produced the best RAPDF scores were selected and used as templates for further optimizations. We had a number of the most promising predicted peptides synthesized for experimental analysis, using the peptide synthesis service from Genemed Synthesis (San Antonio, TX) and CEM Corporation (Matthews, NC) for this (Hrobowski et al., 2005). The computational work was done in collaboration with Ram Samudrala in the Center for Computational Biology at the University of Washington, Seattle.

Experimental analysis of the peptides consisted of in vitro virus inhibition assays using immunostaining plaque reduction assays as described (Hrobowski et al., 2005; Rees et al., 2008). We also tested for inhibitor toxicity to insure that any observed anti-viral activity was not due to target cell killing. We confirmed their activity as entry inhibitors by adding the inhibitors after virus infection has occurred, and assayed for post binding inhibition by adding the inhibitors after virus has bound to the cells at 4^{o}C. We also tested for inhibition of virus:cell binding using a qRT-PCR cell:virus binding assay.

To complement rational computational predictions, we have also made progress on the use of phage display technology to screen peptide mutant libraries and select for enhanced binding variants. A commercially available T7 phage display system (T7 Select, Novagen) is being used to express peptides as C-terminal fusions of the phage capsid protein. The T7 system is ideal because it can accommodate long peptide sequences expressed in an unconstrained manner. Other phage systems can only accommodate short (10-15 aa) sequences as an internal loop in the phage capsid protein. We have engineered a short glycine rich amino acid sequence between the end of the capsid and the inhibitory peptide to provide a flexible linker region and allow the peptides to interact freely with E protein targets. We have previously chemically

modified the N-terminus of peptides DN59, DN57opt and 10AN1 with biotin or fluorescent tags without substantial loss of target binding or inhibitory activity. We have cloned the peptides into the T7Select 10-3b construct that results in an average of 5-15 peptide domains per phage. This provides an intermediate level of peptide presentation for selection. We have characterized the properties of the phage expressing the dengue inhibitory peptides and are now able to proceed with selection experiments on mutagenized peptide sequences.

Peptides are often difficult to develop into clinically useful therapeutics. However, the delivery, stability, and bioavailability of peptides can often be improved through chemical modification of the original peptide structure. With potential future in vivo uses in mind, we proposed to investigate the effects that some modifications may have on the in vitro activity of inhibitory peptides. We have focused on the characterization of retro-inverso peptide mimics where the amino acids are all changed from naturally occurring L-amino acids to non-naturally occurring D-amino acids, and the amino acid order is reversed. This results in a peptide with a backwards peptide backbone, but with similar chirality of the amino acid side chains. Because of the D-amino acid side chains, retro-inverso peptides are typically resistant to degradation and have improved pharmacological properties.

Real time binding assays between peptides and purified DENV E proteins were also performed using biolayer interferometry with an Octet QK system (Fortebio, Menlo Park, CA). This system quantifies light interference on the surface of a fiber optic sensor to measure the thickness of molecules bound to the surface. Targets of interest are chemically tethered to the surface of the sensor using biotin-streptavadin interactions. Binding of a partner molecule to the tethered target molecule results in increased thickness of the surface, which is monitored in real time by changes in the interference of reflected light at the sensor interface. This system generates kinetic on and off rates as well as thermodynamic dissociation constants for binding affinity comparisons.

Peptides were either purchased with an N-terminal biotin tag, or were specifically N-terminally biotinylated at pH 6.5 overnight at 4^{o}C using a 1:1 molar ratio of NHS-LC-LC-Biotin or NHS-PEG4-Biotin (Pierce/ThermoFisher, Rockford, IL) and dialyzed against PBS to remove unreacted biotinylation reagent. Biotinylated peptides were tethered to kinetics grade streptavidin high binding biosensors (Fortebio, Menlo Park, CA) at several different concentrations. Peptide concentrations that gave an interference signal between 0.8 and 1.2 nm binding to the sensor surfaces within 200 s were used for E protein binding studies. Tethered peptides were allowed to bind to and dissociate from several different concentrations of purified, recombinant, DENV 1-4 E proteins obtained from Hawaii Biotechnology (Honolulu, HI). Binding and dissociation kinetics were calculated using the Octet QK software package, which fits the observed binding and dissociation curves to a 1:1 binding model to calculate the kinetic rate constants. Association and dissociation rate constants were calculated using at least two different concentrations of E protein. Thermodynamic dissociation constants were calculated as the kinetic dissociation rate constant divided by the kinetic association rate constant.

Methods, Assumptions, and Procedures

1.1 Peptide computational predictions

Computational optimization of hinge region inhibitory peptides. Peptide inhibitors were designed to have improved in situ binding compared to naturally occurring sequences using the residue-specific all-atom probability discriminatory function (RAPDF) (Huang et al., 2000,

Samudrala et al., 1998). The x-ray diffraction structure of DENV-2 envelope protein (Protein Data Bank identifier 1OAN1) was used as a template for creating mutant structures from which the peptides were derived (Modis et al., 2003). For each peptide, we randomly selected a residue side chain and substituted it with a new side chain. The substitution was performed using a backbone-dependent side chain rotamer library and a linear repulsive steric energy term provided by SCWRL version 3.0 (Bower et al., 1997). The resulting all-atom models were energy minimized for 200 steps using the Energy Calculation and Dynamics (ENCAD) program (Levitt, 1974; Levitt, 1983; Levitt et al., 1969). RAPDF scores were then calculated to estimate the structural stability of a given E protein structure derivative. For a selected residue, side chain substitution was carried out ten times. The amino acid that produced the best RAPDF score was selected and used as a template for further mutation. The entire mutation process was repeated 100,000 times to enable a rigorous search for peptides that produced the best RAPDF score (i.e., highest predicted stability).

Computational design of novel inhibitory peptides. A 20 residue acid sliding window that moved from the N to the C terminus of the E protein in 10 residue acid increments was evaluated by a structural stability (pseudoenergy) optimization protocol using the RAPDF. A Metropolis Monte Carlo search algorithm (Metropolis et al., 1953) was used to change each amino acid in the 20 residue window to one of the other 19 naturally occurring amino acids, and the stability of corresponding peptide in the context of the entire E protein structure was evaluated. This process was iterated 100,000 times using RAPDF as the target scoring function. The Metropolis criterion was used to select a particular change in the simulation: if a particular change resulted in a better RAPDF score (lower pseudoenergy), then it was retained. If a particular change resulted in a worse RAPDF score (higher pseudoenergy), then a random choice, based on the score difference between the previous change and the current one, was made to retain the corresponding change. This procedure enables not only enables design of peptides that will result in high structural and binding stability (i.e., the best RAPDF scores/pseudoenergies), but also enables surmounting local minima encountered during the search. Computational optimization was performed on the four regions corresponding to the best RAPDF score, and therefore the highest binding potential, within the E protein as described above to generate variant peptides sequences.

Viruses and cells. DENV-2 strain NG-C was obtained from R. Tesh at the University of Texas at Galveston. Virus was propagated in the *Macaca mulatta* kidney epithelial cell line, LLC-MK2 (ATCC catalog number CCL-7). Cells were grown in Dulbecco's modified eagle medium (DMEM) with 10% (v/v) fetal bovine serum (FBS), 2 mM Glutamax, 100 U/ml penicillin G, 100 µg/ml streptomycin and 0.25 µg/ml amphotericin B, at 37°C with 5% (v/v) CO_2.

Peptides. Peptides were synthesized by solid-phase N-α-9-flurenylmethyloxycarbonyl chemistry, purified by reverse-phase high performance liquid chromatography and confirmed by amino acid analysis and electrospray mass spectrometry (Genemed Synthesis, San Antonio, TX). Peptide stock solutions were prepared in 20% (v/v) dimethyl sulfoxide (DMSO): 80% (v/v) H_2O, and concentrations determined by absorbance of aromatic side chains at 280 nm.

Focus-forming unit assay. LLC-MK2 target cells were seeded at a density of 1 $x10^5$ cells in each well of a 6-well plate 24 h prior to infection. Approximately 200 focus forming units (FFU) of virus were incubated with or without peptide in serum-free DMEM for 1 h at room temperature. Virus/peptide or virus/control mixtures were allowed to infect confluent target

cell monolayers for 1 h at 37°C, with rocking every 15 min, after which time the medium was aspirated and overlaid with fresh DMEM/10% (v/v) FBS containing 0.85% (w/v) Sea-Plaque Agarose (Cambrex Bio Science, Rockland, ME) without rinsing. Cells with agar overlays were incubated at 4°C for 20 min to set the agar. Infected cells were then incubated at 37°C with 5% CO_2 for 5 days. Infected cultures were fixed with 10% formalin overnight at 4°C, permeablized with 70% (v/v) ethanol for 20 min, and rinsed with phosphate buffered saline, pH 7.4 (PBS) prior to immunostaining. Virus foci were detected using a specific mouse mAb from hybridoma E60 (obtained from M. Diamond at Washington University), followed by horseradish peroxidase-conjugated goat anti-mouse immunoglobulin (Pierce, Rockford, IL), and developed using AEC chromogen substrate (Dako, Carpinteria, CA). Results are expressed as the average of at least two independent trials with three replicates each. IC_{50} values were determined using variable slope sigmoidal dose-response curve fits with GraphPad Prism 4.0 software (LaJolla, CA), except for DN57opt, which was determined graphically due to a lack of data points to produce a reasonable curve fit.

Toxicity assay. Cytotoxicity of peptides was measured by monitoring mitochondrial reductase activity using the TACS™ MTT cell proliferation assay (R&D Systems, Inc., Minneapolis, MN) according to the manufacturer's instructions. Dilutions of peptides in serum-free DMEM were added to confluent monolayers of LLC-MK2 cells in 96-well plates for 1 h at 37°C, similar to the focus forming inhibition assays, and incubated at 37°C with 5% (v/v) CO_2 for 24 h. Absorbance at 560 nm was measured using a Tecan GeniosPro plate reader (Tecan US, Durham, NC).

Post-infection treatment focus forming unit assay. Approximately 200 FFU of DENV-2 without peptide was allowed to bind and enter target cells for 1 h at 37°C as described for the focus forming unit assay. Unbound virus was then removed by rinsing with PBS and peptide was added to the cells for 1 h at 37°C. Cultures were washed again in PBS and agarose overlays, incubation, and immunological detection was conducted as described for the focus forming unit assay.

Virus:cell binding inhibition assay. Binding inhibition assays were modified from Thaisomboonsuk et al., 2005. Briefly, LLC-MK2 monolayers were rinsed in 4°C DMEM containing 0.8% BSA and 25mM HEPES, pH7.5. Virus was incubated at 4°C with peptides, control anti-dengue serum, or heparan sulfate in DMEM/BSA/HEPES for one hour before adding to the monolayers for 2 hours at 4°C. Monolayers were rinsed 3 times with cold DMEM/BSA/HEPES media prior to RNA extraction using the Qiagen RNeasy mini kit (Valencia, CA) per manufacturer's instructions. Quantitative, real time, reverse transcriptase polymerase chain reaction (qRT-PCR) was conducted utilizing the Roche Lightcycler RNA Master SYBR Green 1 qRT-PCR kit (Basel, Switzerland), using primers Den_F (TTAGAGGAGACCCCTCCC) and Den_R (TCTCCTCTAACCTCTAGTCC) from Chutinimitkul et al., 2005 and the following cycling conditions: 1 h at 61°C, 30 s at 95°C, followed by 45 cycles of: 5 s at 95°C, 20 s at 61°C, and 30 s at 72°C. Cp values were used to estimate infectious units according to a standard curve. Independent assays were repeated three times, in duplicate or triplicate.

1.2 Peptide phage display – mutagenesis and selection studies

Construction of T7 phage expressing DENV inhibitory peptides. The Novagen (EMD Chemicals, Gibbstown, NJ) T7 select phage display system was used to clone DNA

sequences coding for the DN59, DN57opt, and 1OAN1 inhibitory peptides as fusion proteins at the C-terminus of the phage capsid protein. The mid-level (select 10-3b) expression construct was used in order to obtain approximately 5-15 capsid:peptide fusion proteins per phage. Additional wild type phage with no fusion insert, and phage with a streptavidin tag fusion were produced as controls. The fusion protein insert regions were amplified and sequenced to confirm correct construction. Clonal phage stocks were grown, purified, titered, and aliquoted for further use. To assay for specific binding of the peptide-expressing phage, an ELISA was constructed using a Ni^{+2} coated 96 well plate, polyhistidine tagged purified dengue-2 E protein, followed by phage, a mouse anti-phage monoclonal antibody, and an HRP-conjugated goat ant-mouse secondary antibody. Color was developed with tetramethylbenzidine-peroxide as substrate for peroxidase. The reaction was stopped after 4 minutes by adding 1% phosphoric acid and color was read as optical density (OD) at 450nm.

1.3 Peptide modifications

Peptides. Peptides were synthesized by solid-phase N-α-9-flurenylmethyloxycarbonyl chemistry, purified by reverse-phase high performance liquid chromatography and confirmed by amino acid analysis and electrospray mass spectrometry (Genemed Synthesis, San Antonio, TX). Peptide stock solutions were prepared in 20% (v/v) dimethyl sulfoxide (DMSO): 80% (v/v) H_2O, and concentrations determined by absorbance of aromatic side chains at 280 nm.

1.4 Biolayer interferometry binding studies of peptides

Peptide:E protein biolayer interferometry binding assay. Real time binding assays between peptides and purified DENV-2 S1 E protein were performed using biolayer interferometry on an Octet QK system (Fortebio, Menlo Park, CA). This system monitors interference of light reflected from the surface of a fiber optic sensor to measure the thickness of molecules bound to the sensor surface. Purified, recombinant, 80% truncated DENV-2 S1 E protein was obtained from Hawaii Biotechnology (Honolulu, HI). Peptides were N-terminally biotinylated with a 5:1 molar ratio of NHS-LC-LC-Biotin (Pierce/ThermoFisher, Rockford, IL) in PBS pH 6.5 at 4°C. Excess biotinylation reagent was removed using Pepclean C-18 spin columns (Pierce/ThermoFisher, Rockford, IL). Biotinylated peptides were coupled to kinetics grade streptavidin high binding biosensors (Fortebio, Menlo Park, CA) at several different concentrations. Sensors coated with peptides were allowed to bind to E protein in PBS with 0.02% (v/v) Tween-20 and 1 mg/ml BSA at several different E protein concentrations. Binding kinetics were calculated using the Octet QK software package, which fit the observed binding curves to a 1:1 binding model to calculate the association rate constants. E protein was allowed to dissociate by incubation of the sensors in PBS. Dissociation curves were fit to a 1:1 model to calculate the dissociation rate constants. Binding affinities were calculated as the kinetic dissociation rate constant divided by the kinetic association rate constant.

Results and Discussion

We have successfully used computational approaches to develop three peptides that inhibit DENV infectivity. DN59, a peptide mimicking the stem region of the DENV E protein shows broad inhibitory activity against all four serotypes of DENV (Figure 1). DN57opt and 1OAN1 peptides were designed to displace regions in the DENV E protein domain I/II regions and show specific inhibitory activity against DENV-2, while sequence scrambled versions of these peptides do not show inhibitory activity (Figures 2 and 3). We have made excellent progress in setting up and testing a phage display system expressing inhibitory peptides that can

be used to select for higher affinity binding peptides (Figure 4). We have designed and tested a modified inhibitory peptide consisting of all D amino acids and have found that it retains its inhibitory activity (Figure 5). We have quantified the affinities of these peptides using a label free biolayer affinity system and derived on and off binding and dissociation kinetic rate constants and equilibrium affinity constants (Figure 6).

1.1 Peptide computational predictions

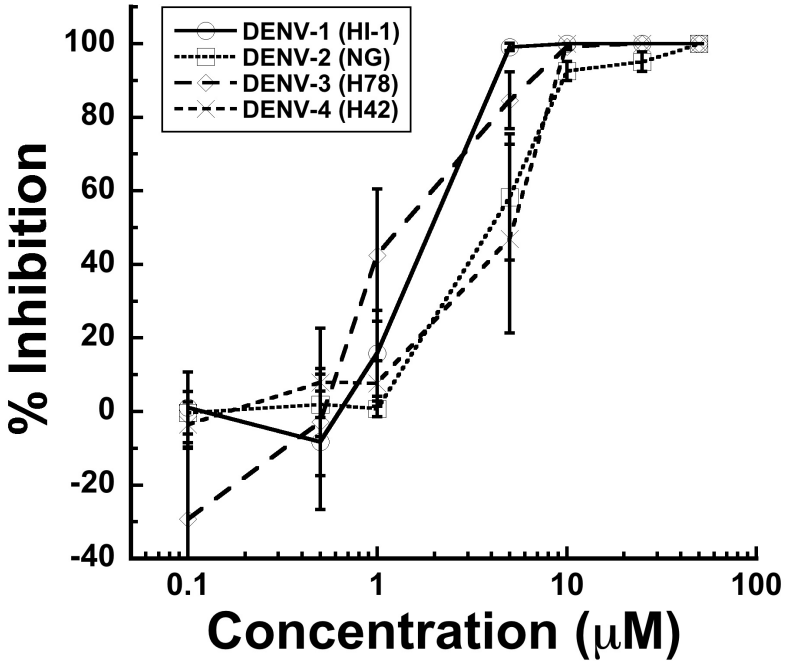

Figure 1: DENV inhibition by DN59 peptide.
The DN59 peptide which mimics a portion of the stem region of the DENV-2 E protein shows dose-responsive inhibition against all four serotypes of DENV in a focus forming reduction assay.

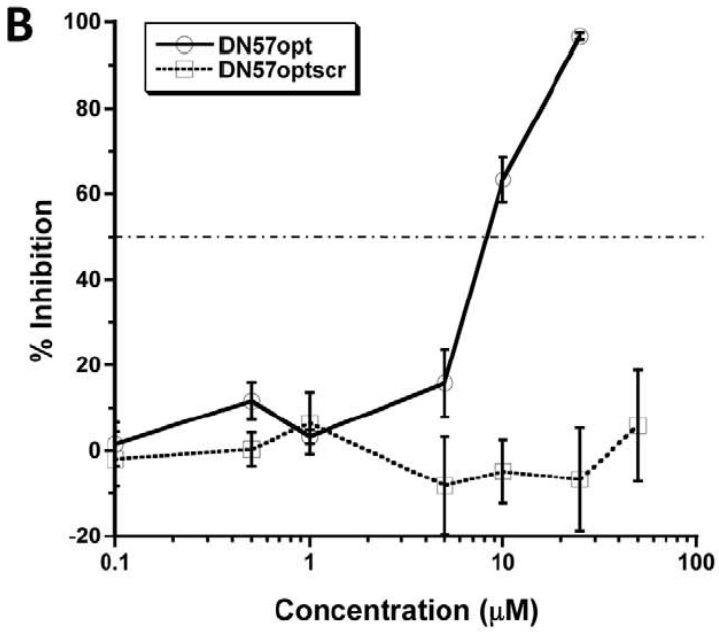

Figure 2: DENV inhibition by DN57opt and corresponding scrambled peptide of identical composition.

Increasing concentrations of DN57opt peptide and corresponding scrambled peptide of identical composition were tested against DENV-2 in a focus forming unit reduction assay. Only the DN57opt peptide shows evidence of inhibitory activity (Costin et al., 2010).

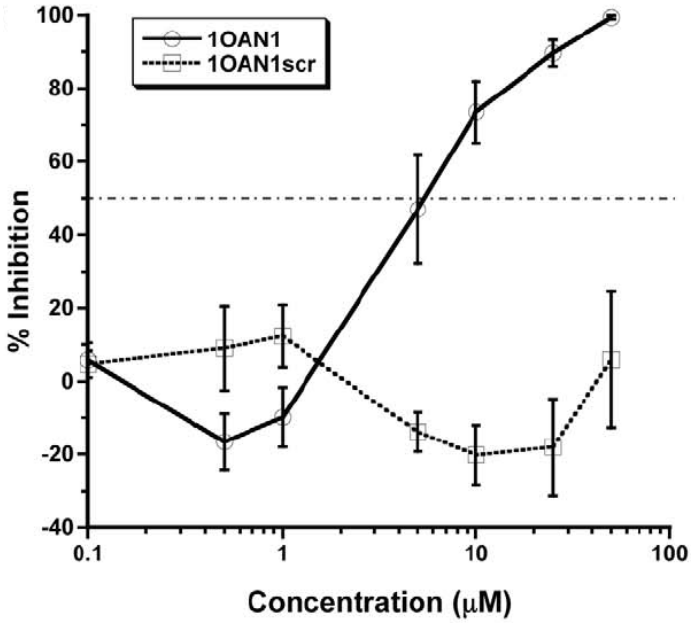

Figure 3: DENV inhibition by 1OAN1 and corresponding scrambled peptide of identical composition.

Increasing concentrations of 1OAN1 peptide and corresponding scrambled peptide of identical composition were tested against DENV-2 in a focus forming unit reduction assay. Only the 1OAN1 peptide shows evidence of inhibitory activity (Costin et al., 2010).

1.2 Peptide phage display – mutagenesis and selection studies

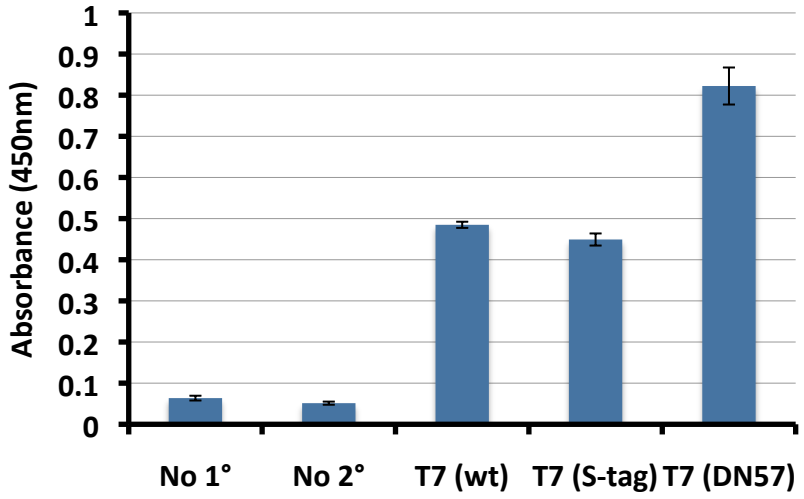

Figure 4: ELISA showing specific binding of peptide expressing phage to DENV E protein. Ni^{+2} plates were coated with polyhistidine tagged DENV-2 E protein and bound to either a T7 phage expressing the DN57opt peptide (DN57), or control phage expressing a streptavidin tag (S-tag), or no tag (wt). Bound phage was detected with a mouse monoclonal antibody against the T7 phage, followed by a secondary goat anti-mouse antibody conjugated to HRP. HRP was detected with TMB substrate. The results show specific binding of the DN57opt expressing phage.

1.3 Peptide modifications

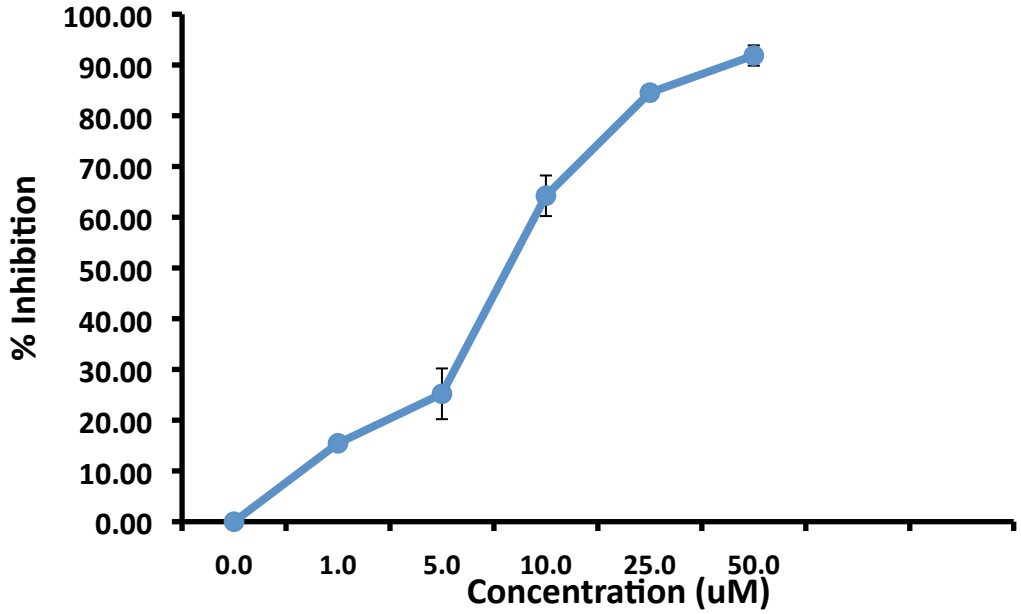

Figure 5: DENV inhibition by RI57.

A "retro-inverso" modified version of the DN57opt peptide retains inhibitory activity against DENV-2 in a focus forming unit reduction assay. This modified peptide was synthesized by reversing the amino acid sequence and converting all of the amino acids to the D chirality. This modified peptide should be physiologically inert to degradation when used as a drug due to having a non-natural chirality.

1.4 Biolayer interferometry binding studies of peptides

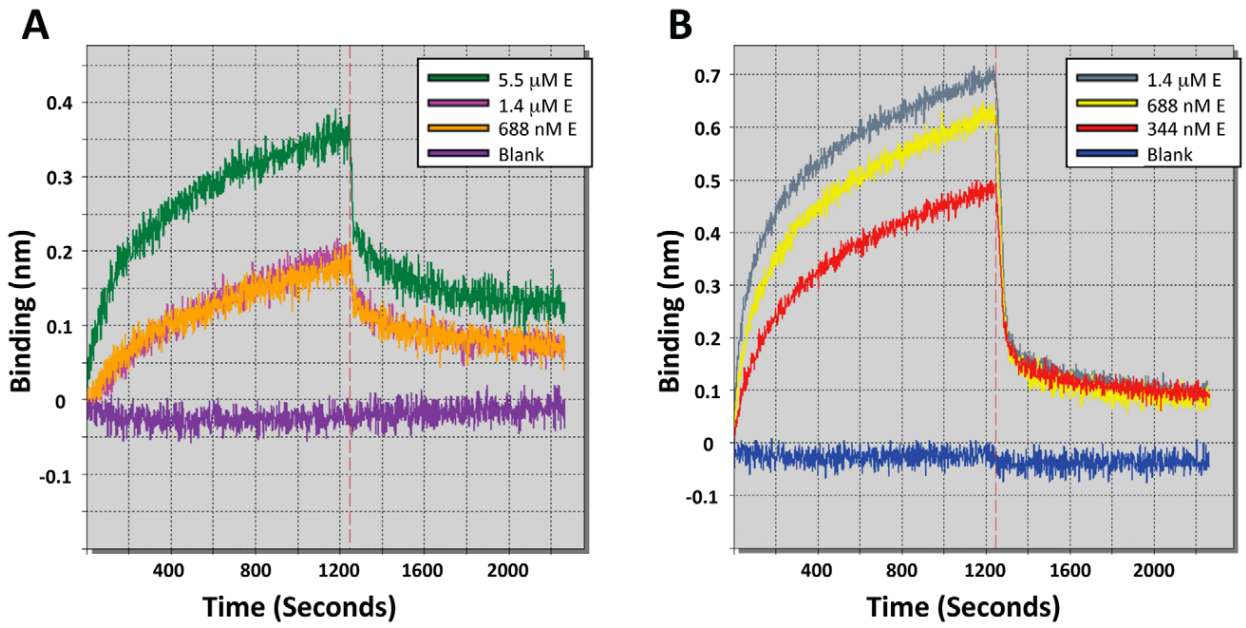

Figure 6: Peptide:E protein binding assay.
Biolayer interferometry was used to assay the binding of the peptides to truncated E Protein. The association and dissociation of increasing concentrations of truncated E protein to peptides DN57opt (A) and 1OAN1 (B) are shown. A buffer blank (PBS, 0.02% Tween-20, 0.1% BSA) containing no E protein was run for each peptide. The affinity of the peptides for the truncated E protein was calculated (DN57opt K_D = $1.2x10^{-6}$ +/- $0.6x10^{-6}$ M (mean+/-sd), 1OAN1 K_D = $4.5x10^{-7}$ +/- $2.0x10^{-7}$ M) (Costin et al., 2010).

Conclusions

We have designed and characterized three different kinds of DENV inhibitory peptides and published two peer-reviewed manuscripts describing their activities (Costin et al., 2010; Nicholson et al., 2011). Additional manuscripts are currently submitted and also in preparation. These peptides are lead compounds for development of clinically useful antivirals against the most problematic insect transmitted virus disease. We have further developed a phage display system to select for inhibitory peptides with greater binding affinity, and we have chemically modified our peptide inhibitors to have greatly improved pharmacological properties. As far as we are aware, our development of the retro-inverso DN57opt peptide represents the first discovery of a retro-inverso antiviral. We have investigated and quantified the affinities between our inhibitory molecules and their specific virus target proteins, which will enable us to characterize in great detail the differences in target affinity of future peptide modifications.

Task 2: Peptide inhibitor resistance

Introduction

Information regarding specific mutations that confer resistance to antivirals reveals details of the structural interactions between the inhibitor and the target protein as well as the mechanism of action of the inhibitor. To investigate this, we have grown viruses in the presence of inhibitory peptides at either constant concentrations of inhibitory peptide or with increasing concentrations at every passage. At intervals, the passaged virus has been tested using a plaque reduction assay for any changes in sensitivity to the inhibitor. We have identified the signature loss of inhibitor sensitivity that results from resistance mutations and we are now pursuing the characterization of these mutations.

Methods, Assumptions, and Procedures

In order to identify how inhibitory peptides might induce viral resistance to inhibition in the E protein, DENV-2 NG-C was passaged ten times over the course of 30 days in the presence of peptide inhibitor. At each passage the virus was incubated with a sufficiently high concentration of DN59, DN57opt or 1OAN1 to inhibit 95% of wild type virus. The 10th and final passage was evaluated for phenotypic and genetic changes in the prM/M and E protein. Selected virus populations were compared to wild type control virus populations for sensitivity to inhibition using a plaque reduction assay. Viral RNA was extracted from cell culture supernatants and reverse transcribed into cDNA. The cDNA was amplified via PCR with gene specific primers for the PrM and E protein region. PCR products were verified via gel electrophoresis and then sequenced. Sequence data was assembled, aligned with a non-selected but passaged control sequence and analyzed for mutations.

Results and Discussion

We have successfully selected DENV populations for phenotypic evidence of reduced sensitivity to inhibitory peptides. We anticipate that sequence analysis of these virus populations will identify mutations that will shed light on the mechanism(s) of this resistance and lead to novel ideas for second generation inhibitory molecules.

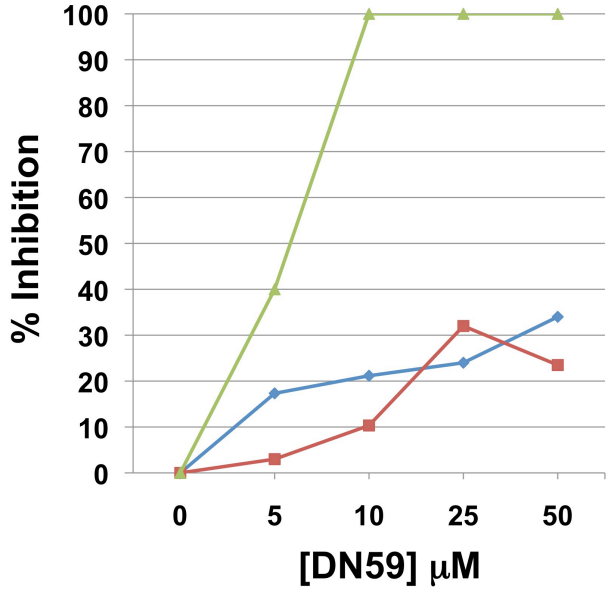

Figure 7: Selection against an inhibitory peptide (DN59) results in a phenotypic change indicative of loss of sensitivity to inhibitor.
DENV-2 was passaged for ten rounds in the presence of high concentrations of the DN59 inhibitory peptide. The resulting virus populations were then assayed for sensitivity to inhibition with increasing amounts of DN59. The virus from two different selection experiments (red and blue) is shown compared to the control virus in green. The selected virus populations show reduced sensitivity to the effects of the inhibitor.

Conclusions

Virus replication machinery is highly error prone and virus populations thus exist as swarms of highly diverse genetic relatives. Selection pressure in the form of some type of inhibitor will shift the population towards the survival of genetic variants that resist the activity of the inhibitor. We have selected DENV populations with our inhibitors and can show phenotypic evidence of a shift towards reduced inhibitor sensitivity. Characterizing the resulting mutants will reveal details of the mechanism of the original inhibitory pressure as well as provide insight into how to design inhibitors that will be active against the resistant mutants.

Task 3: Expression of peptide inhibitors in transgenic mosquitoes

Introduction

A potentially powerful approach to the control of vector born viruses is to genetically modify the vector populations to render them incapable of transmitting these viruses. One of the pathogen binding, inhibitory peptides that we have previously developed (DN59) targets a highly conserved region of the dengue virus surface envelope glycoprotein. This region is conserved among all known flaviviruses, including dengue, West Nile, yellow fever, Saint Louis encephalitis, Japanese encephalitis, and tick borne encephalitis viruses. We proposed to develop this technology to create genetically resistant insects that could be released to compete with local insect vectors and result in populations that are incapable of transmitting pathogenic viruses.

We have confirmed that this peptide inhibits flavivirus infection in mosquito cells in vitro. However, we have been unsuccessful in expressing this peptide in any system, due to problems with the post expression stability of the peptide.

Methods, Assumptions, and Procedures

3.1 Peptide inhibition in mosquito cell line

Virus inhibition on mosquito C6/36 cells. C6/36 monolayers were infected with approximately 7600 FFU of DENV-2 at 37°C for 1 h before being aspirated, complete culture media added, and incubated at 37°C and 5% CO_2. After 72 h, RNA was isolated from cells using an RNeasy Mini Kit (Qiagen, Valencia, CA). qRT-PCR was performed as previously described (Chutinimitkul et al., 2005).

3.2 Expression of peptides in Sindbis system

Expression of peptide fusion proteins. Expression of DN59 peptide was performed in E. coli as a fusion protein with maltose binding protein, under the control of an inducible lac promoter. Expression of DN59 peptide was performed in human 293T cells as a fusion with green fluorescent protein under the control of the constitutive cytomegalovirus immediate early promoter.

Results and Discussion

We have shown that the activities of our peptide inhibitors are not cell type dependent and that they can function to inhibit infection in mosquito cells. We attempted to express the peptides as fusion proteins, but were unable to generate high enough expression levels. We speculate that this is due to the low stability of these peptides as fusion proteins. This is a common problem with expressed proteins.

3.1 Peptide inhibition in mosquito cell line

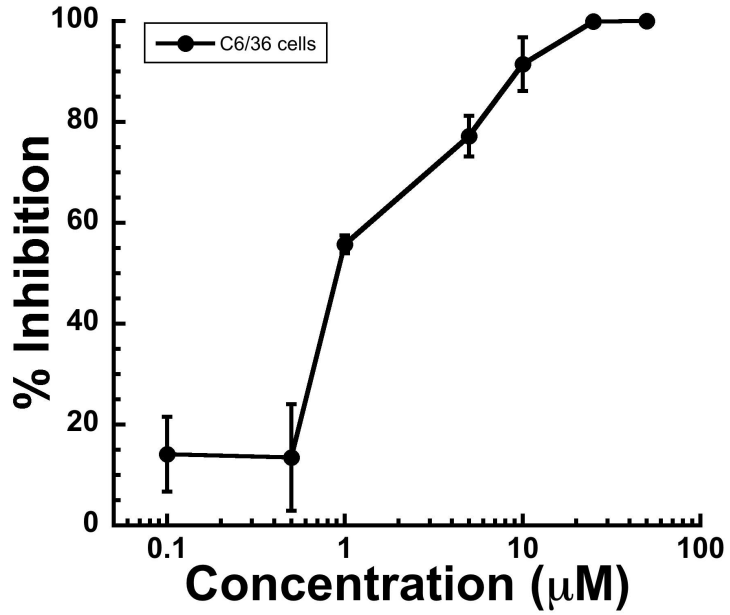

Figure 8: Focus forming unit reduction assay showing dose response inhibition of infection of DENV-2 in mosquito cells (C6/36).
Increasing concentrations of the DN59 peptide inhibit DENV-2 infection into mosquito C6/36 cells, indicating that the peptide activity is not cell line dependent.

3.2 Expression of peptides in Sindbis system

Conclusions

Our DENV inhibitory peptides are active against virus infection in mosquito cells, confirming our hypothesis that expression of peptides in mosquitoes may lead to inhibition and inability to transmit virus. Unfortunately, we have been unsuccessful in expressing sufficient quantities of peptides in any expression system.

Task 4: Anti-dengue human monoclonal antibodies

Introduction

Our previous experience with anti-viral binding and entry inhibition peptides and small molecules has lent insight into the requirements for successful vaccine strategies against difficult viral targets. We originally proposed the rational design of novel vaccines against viral targets where previous vaccine strategies have resulted in increased pathogenicity. Despite success with

a limited number of pathogens, vaccines for some of the worst viral diseases still do not exist. In some cases anti-viral vaccines have even been shown to enhance illness. We have used the dengue virus system to identify specific human antibody responses that neutralize virus versus specific antibody responses that result in antibody-mediated enhancement (ADE) of infection (Halstead, 2003). We had previously obtained IRB approval and collected and stored in liquid nitrogen serum and peripheral blood mononuclear cells (PBMCs) from recovered DENV patients from Singapore and Jamaica. In collaboration with James Robinson at Tulane University, we have used Epstein-Barr virus transformation to produce and characterize of the first human monoclonal antibodies (hMAbs) that specifically recognize the DENV E protein.

To determine the specificity (reactivity with DENV 1, 2, 3, and/or 4) of the hMabs, ELISA assays were performed with antigens from each of the four serotypes of dengue. To determine whether the hMAbs inhibit the infection of specific DENV strains, virus neutralization assays were performed with each of the four serotypes of dengue. Infection enhancement studies were conducted using the human transformed macrophage-like cell line K562. This cell line expresses antibody binding Fc receptors and supports enhanced entry of DENV in the presence of anti-DENV antibodies. Real time binding assays between purified hMAbs and purified DENV E proteins were performed using biolayer interferometry with an Octet QK system (Fortebio, Menlo Park, CA) similarly to the description for inhibitory peptide binding. Association and dissociation rate constants were calculated using at least two different concentrations of antibody. Thermodynamic dissociation constants were calculated as the kinetic dissociation rate constant divided by the kinetic association rate constant. For structural verification, we had proposed to perform three dimensional cryoEM of virus complexed with hMAbs. We report preliminary results showing the symmetrical binding of a HMAb to DENV particles.

Methods, Assumptions, and Procedures

4.1 HMAb ELISAs

Viruses and Cells. DENV-1 strain HI-1, DENV-2 strain NG-2, DENV-3 strain H-78, and DENV-4 strain H-42, were obtained from R. Tesh at the World Health Organization Arbovirus Reference Laboratory at the University of Texas at Galveston. Viruses were propagated in the Macaca mulatta kidney epithelial cell line, LLC-MK2, obtained from the ATCC (Manassas, VA). LLC-MK2 cells were grown in Dulbecco's modified eagle medium (DMEM) containing 10% (v/v) fetal bovine serum (FBS) 2mM Glutamax, 100 U/ml penicillin G, 100µg/ml streptomycin and 0.25 µg/ml amphotericin B, at 37°C with 5% (v/v) CO_2. The cells were inoculated with dengue virus stock at 70% to 80% confluency, cultured in DMEM and 10% FBS for seven days, at which time medium was changed to Protein Free Hybridoma Medium (Gibco, Carlsbad, CA). After ten days in culture, supernatant fluids were collected and treated with 1% Triton-X 100 to solubilize and inactivate virus. Adherent cells were collected by treatment with trypsin-EDTA for three minutes. Cells were then pelleted by centrifugation at 1000 rpm for 10 minutes. The pellet was re-suspended in 5 ml of PBS containing 1% Triton-X 100. The detergent treated preparations were then mixed thoroughly and aliquoted and frozen at -20ºC for later use. K-562 hematopoietic cells (ATCC, Manassas VA), used for virus enhancement assays, were grown in RPMI-1640, 10% (v/v) FBS, 2mM Glutamax, 100 U/ml penicillin G, 100µg/ml streptomycin and 0.25 µg/ml amphotericin B, at 37°C with 5% (v/v) CO_2.

Patient Sample. A patient was identified who had been hospitalized in Singapore with a dengue virus infection in April of 2005. The infection was likely acquired while the patient was

traveling in Myanmar. Blood was drawn in September 2007, after informed consent was obtained, and peripheral blood mononuclear cells (PBMCs) were isolated by Ficoll-Hypaque gradient centrifugation and viably frozen in liquid nitrogen. The patient's serum was tested by ELISA and neutralization assays in an attempt to determine the likely infecting serotype. Institutional Review Board approval was obtained for this study at all participating institutions.

Epstein-Barr Virus Transformation. The production of HMAbs by EBV-transformation of B cells has been described elsewhere (Xiang et al., 2002; Robinson et al., 1990a; Robinson et al., 1990b). Briefly, viably cryopreserved PBMCs were thawed, washed in Hank's Buffered Salt Solution, and inoculated with EBV (B95-8 strain). Cells were suspended in RPMI containing 20% FBS, Primacin® (InVivoGen, San Diego, CA) and 2 μg/ml CpG 2006 (Midland Certified Reagent Co., Midland, TX) and plated at 104 cells per well in 96 well tissue culture plates previously seeded with approximately 50,000 irradiated mature macrophages per well derived from PBMC of healthy blood donors which served as "feeder cultures" that promote outgrowth of transformed B cells. Antibody-positive wells that contained growing cells were sub-cultured at several dilutions and re-screened by ELISA. Cell lines that continued to grow and produce antibody during several low cell density passages were finally cloned at limiting dilution. Definitively cloned cell lines were expanded to grow as suspension cultures in stationary 490-cm^2 roller bottle cultures (Corning, Corning, NY) from which cell culture fluid was harvested weekly. HMAbs were purified from one to two liters of culture supernatant by Protein A affinity chromatography. The IgG subclass and light chain type of each antibody was determined by reactivity with MMAbs to the four heavy chain subclasses (Southern Biotech, Birmingham, AL) and polyclonal goat antibodies to kappa and lambda chains by ELISA using established methods.

ELISA to Detect Human and Murine Anti-Dengue Virus Monoclonal Antibodies. Transformed B cell cultures were screened for antibody production using a modification of an immunoassay described previously in which virus envelope glycoproteins are immobilized in wells coated with Concanavalin A (ConA) a plant lectin that binds carbohydrate moieties on glycoproteins of a variety of enveloped viruses (Robinson et al., 1990a). 96-well plates (Costar®, Corning, Corning, NY) were coated with ConA (Vector Laboratories, Burlingame, CA) at 25 μg/ml in 0.01M HEPES (Gibco, Carlsbad, CA) and 100 μl per well for one hour. The wells were washed and solubilized DENV was incubated for one hour. A requirement of this assay is that virus must be grown in serum free medium so that viral glycoproteins can be captured in ConA coated wells. Media containing FBS has glycoproteins that will bind to ConA and block capture of DENV E protein resulting in low OD readings. After a wash step with PBS containing 0.1% (v/v) Triton-X 100, un-reacted ConA binding sites in the wells were blocked with RPMI Medium 1640 and 10% FBS for 30 minutes. Culture fluids from each 96 well culture plate containing EBV transformed B cells were transferred to corresponding wells of assay plates coated with dengue E proteins and incubated for one hour at room temperature. Undiluted supernatant of murine MAb 3H5 (ATCC HB-46), which binds to DENV-2, was used as a positive control during the screening process (Henchal et al., 1985). Negative controls consisted of LLC-MK-2 culture fluid grown in parallel with no virus as well as vaccinia expressed HIV envelope glycoprotein's from the ADA strain of HIV-1 produced in serum free medium. The wells were again washed and then incubated with 100ul of peroxidase-conjugated goat anti-human IgG-gamma (Zymed, San Francisco, CA) or peroxidase-conjugated affinity purified anti-mouse IgG (Rockland, Gilbertsville, PA) diluted 1:2000 in PBS-0.5% (v/v) Tween 10% (w/v)

whey (BiPro, Le Sueur, MN) and 10% (v/v) FBS for one hour. After a final wash step, color was developed with 100µl/well tetramethylbenzidine-peroxide (TMB)-H_2O_2 as substrate for peroxidase. The reaction was stopped after 4 minutes by adding 1% phosphoric acid and color was read as optical density (OD) at 450nm. All steps in this ELISA were performed at room temperature.

4.2 HMAb virus neutralization assays

Focus-forming-unit Reduction Neutralization Titer. LLC-MK-2 target cells were seeded at a density of approximately 500,000 cells in each well of a 12-well plate 24 h prior to virus inoculation. Approximately 100 focus forming units (ffu) of virus were incubated with heat inactivated patient serum or purified HMAb in serum-free DMEM for one hour at room temperature. Virus mixtures were allowed to infect confluent target cell monolayers for one hour at 37°C, with rocking every 15 min, after which time the inoculum was aspirated and overlaid with fresh MEM/10% (v/v) FBS containing 1.2% (w/v) microcrystaline cellulose (Avicel®, FMC, Newark, DE). Infected cells were then incubated at 37°C with 5% CO_2 for two days (DENV-4), three days (DENV-1 and -3), or four days (DENV-2). Infected cultures were fixed with 10% (w/v) formalin overnight at 4°C, permeabilized with 70% (v/v) ethanol for 20 minutes, and rinsed with PBS prior to immunostaining. Virus foci were detected using specific mouse anti-DENV E protein MMAb E60 (obtained from M. Diamond at Washington University), followed by horseradish peroxidase-conjugated goat anti-mouse immunoglobulin (Pierce, Rockford, IL), and developed using AEC chromogen substrate (Dako, Carpinteria, CA). Results are expressed as pooled data from two independent experiments with three replicates each.

4.3 Antibody enhancement of viral entry

Enhancement Assay. Enhancement assays were conducted using DENV-1 in K-562 hematopoietic cells. Varying concentrations of each HMAb were incubated with 7,500 ffu of virus for 1 hour at 37°C in 200 µl of serum free RPMI-1640, then added to 75,000 cells in 300 µl of complete medium in a 24-well plate and incubated at 37°C with 5% CO_2 for 3 days. RNA was extracted from cell lysates using the RNeasy Mini kit (Qiagen, Valencia CA). Quantitative RT-PCR was performed with a DENV-1 specific primer pair (D1S and D1C) that produces a 490 bp product from the NS1 region, using a LightCycler 480 II (Roche, Indianapolis, IN) and a one step LightCycler RNA Master SYBR Green I kit (Roche) (Morita et al., 1991). Amplification conditions were 61°C for 30 min, 95°C for 30 sec, and 45 cycles of 95°C for 5 sec, 61°C for 20 sec, and 72°C for 30 sec.

4.4 Biolayer interferometry binding studies of HMAbs

Biolayer Interferometry Binding Assays. Real time binding assays between purified antibodies and purified DENV E proteins were performed using biolayer interferometry with an Octet QK system (Fortebio, Menlo Park, CA). This system measures light interference on the surface of a fiber optic sensor, which is directly proportional to the thickness of molecules bound to the surface. Targets of interest are chemically tethered to the surface of the sensor using biotin-streptavidin interactions. Binding of a partner molecule to the tethered target results in thickening of the surface, which is monitored in real time. Purified, recombinant, 80% truncated DENV 1-4 E proteins were obtained from Hawaii Biotechnology (Aiea, HI) (Cuzzubo et al., 2001). E proteins were biotinylated for 30 minutes at room temperature using a 5:1 molar ratio of NHS-LC-LC-Biotin (Pierce/ThermoFisher, Rockford, IL) and dialyzed against PBS to remove

unreacted biotinylation reagent. Biotinylated E proteins were coupled to kinetics grade streptavidin high binding biosensors (Fortebio, Menlo Park, CA) at several different concentrations. E protein binding concentrations that gave a signal between 0.8 and 1.2nm binding to the sensor surfaces within 200 seconds were used for antibody binding studies. Unbound E proteins were removed from the surface of the sensors by incubation in PBS. Probes coupled to E protein were allowed to bind to antibodies at several different concentrations, and binding kinetics were calculated using the Octet QK software package, which fit the observed binding curves to a 1:1 binding model to calculate the association rate constants. Antibodies were allowed to dissociate by incubation of the sensors in PBS. Dissociation kinetics were calculated using the Octet QK software package, which fit the observed dissociation curves to a 1:1 model to calculate the dissociation rate constants. Association and dissociation rate constants were calculated using at least two different concentrations of antibody. Equilibrium dissociation constants were calculated as the kinetic dissociation rate constant divided by the kinetic association rate constant.

4.5 CryoEM of virus HMAb complexes

Cryo-electron microscopy of HMAb complexed to dengue virus particles. Fab fragments of the HMAb D11C were prepared by digestion with pepsin and purified by removal of the heavy chain tails using a protein A column. Fab fragments were complexed with gradient purified DENV 2 NG-C particles and subjected to flash freezing and imaging as described (Zhang et al., 2003).

Results and Discussion

We have successfully isolated and characterized a number of human monoclonal antibodies directed against the DENV E protein. This includes antibodies with differential recognition of DENV serotypes as well as broadly reactive antibodies (Figure 9). Some of these antibodies have been isolated from donors with serotype specific serum responses, others from donors with broadly reactive serology (Figure 10). Some antibodies that interact with DENV E protein do not neutralize virus infectivity (Figures 11 and 12). Others show infection neutralization activity against more than one, or all four serotypes (Figures 13, 14, and 15). All human monoclonal antibodies tested to date show evidence of inducing antibody-dependent enhancement (ADE) of DENV infection into Fc receptor-bearing, macrophage like cell lines. This can correlate with increased disease severity. Monoclonal antibodies that do not neutralize infections show ADE that increases with increasing concentration and stays high, while monoclonal antibodies that have neutralizing activity show ADE that increases up to a point and then declines at higher concentrations (Figure 16). This decline is especially noticeable with highly neutralizing antibodies (Figures 17, 18, 19, and 20). We have used Octet biolayer interferometry to analyze the on and off rates and binding affinities of a number of monoclonal antibodies (Figure 21 and Table 1). In general, human monoclonal antibodies are higher affinity than murine monoclonals. In collaboration with Dr. Shee Mei Lok at Duke-NUS in Singapore, we have begun to structurally characterize how these human monoclonal antibodies bind to DENV particles using cryo electron microscopy (Figure 22).

4.1 HMAb ELISAs

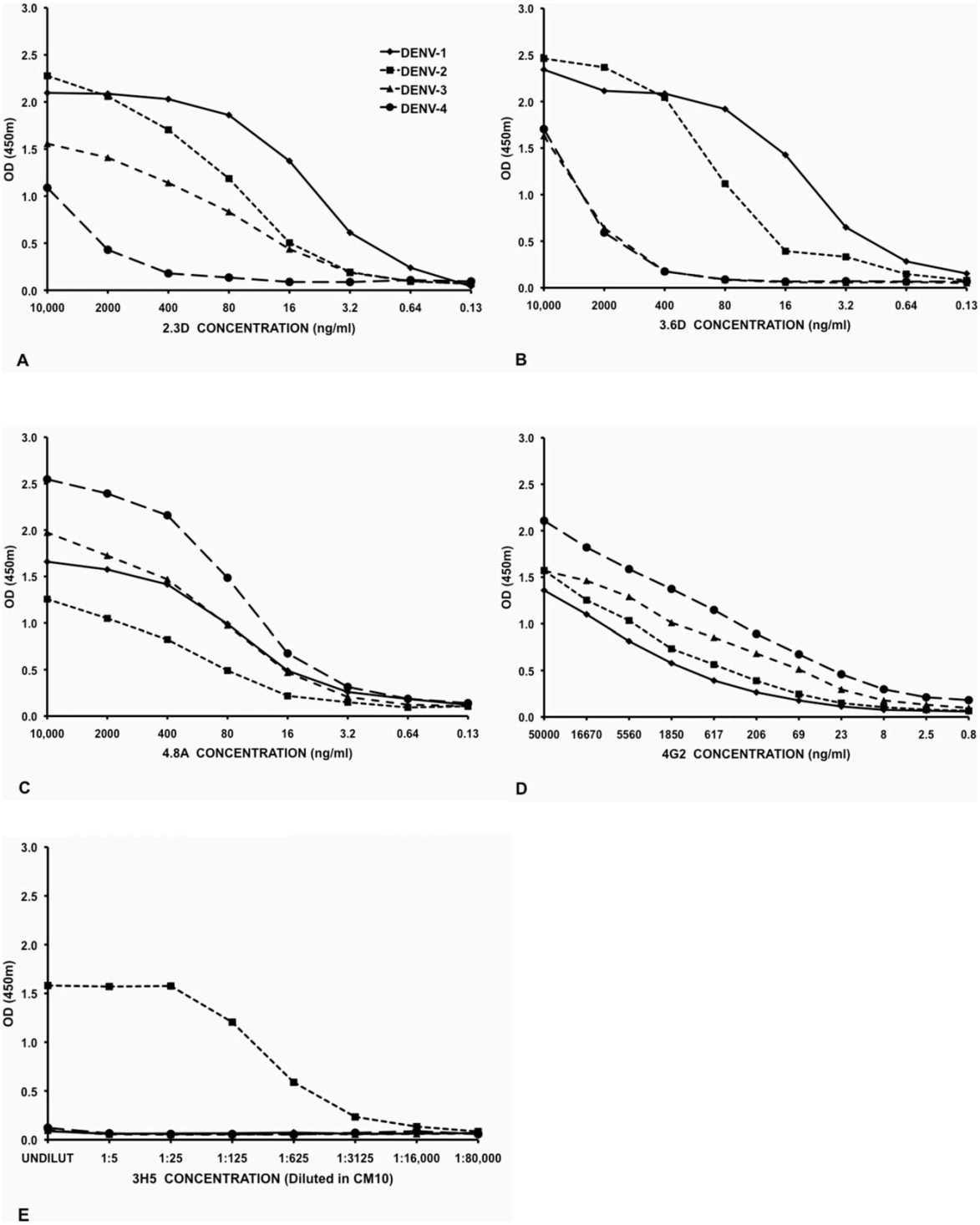

Figure 9: ELISAs with serial five fold dilutions of each HMAb.
Starting at 10,000 ng/ml, Human and Mouse MAbs were tested by ConA ELISA against each dengue virus serotype. A HMAb 2.3D. B 3.6D. C 4.8A. D. 4G2 (dilutions were started at 50,000 ng/ml). E. 3H5 (tested as dilutions of culture fluid) (Schieffelin et al., 2010).

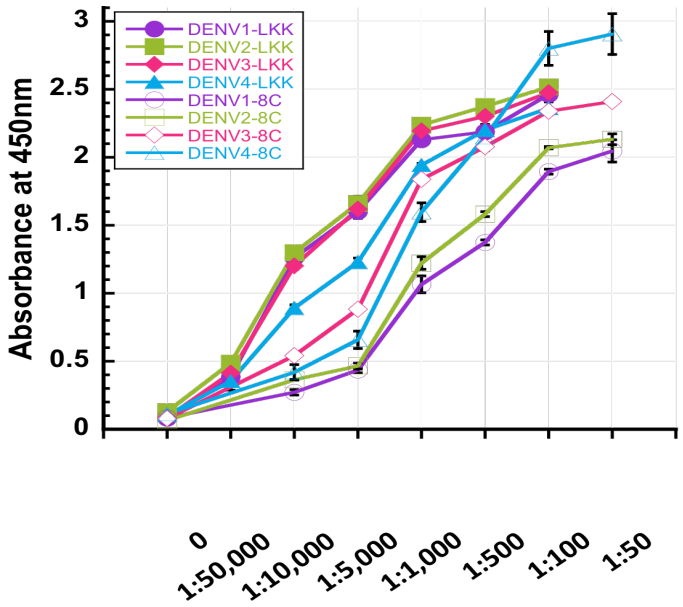

Figure 10: ELISAs of patient sera show broad neutralization of all four serotypes of DENV.

4.2 HMAb virus neutralization assays

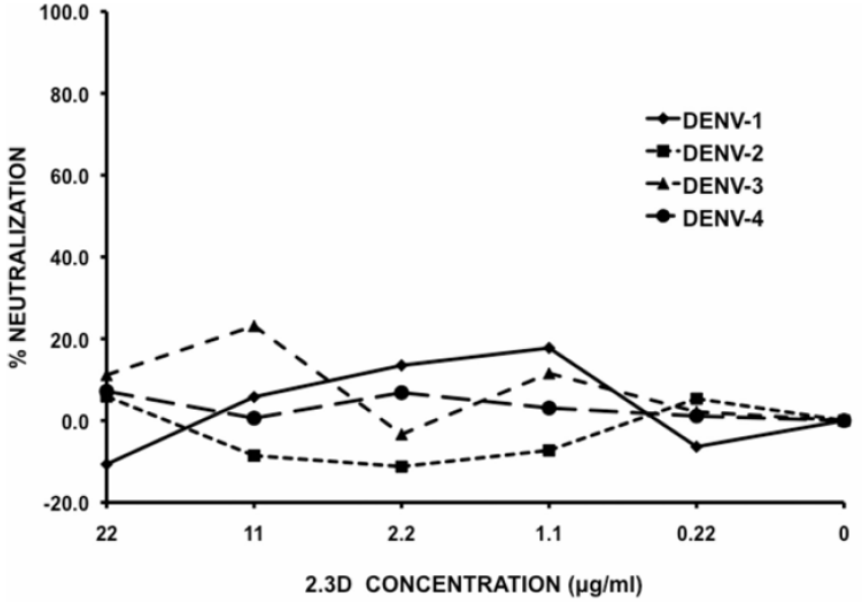

Figure 11: DENV is not neutralized by the 2.3D HMAb.
Approximately 100 FFU of virus were incubated with serial dilutions of purified monoclonal antibody 2.3D. Virus mixtures were allowed to infect LLC-MK2 cells and then incubated at 37°C. Virus foci were detected using anti-DENV E protein MMAb E60. Results are expressed as pooled data from two independent experiments with three replicates (Schieffelin et al., 2010).

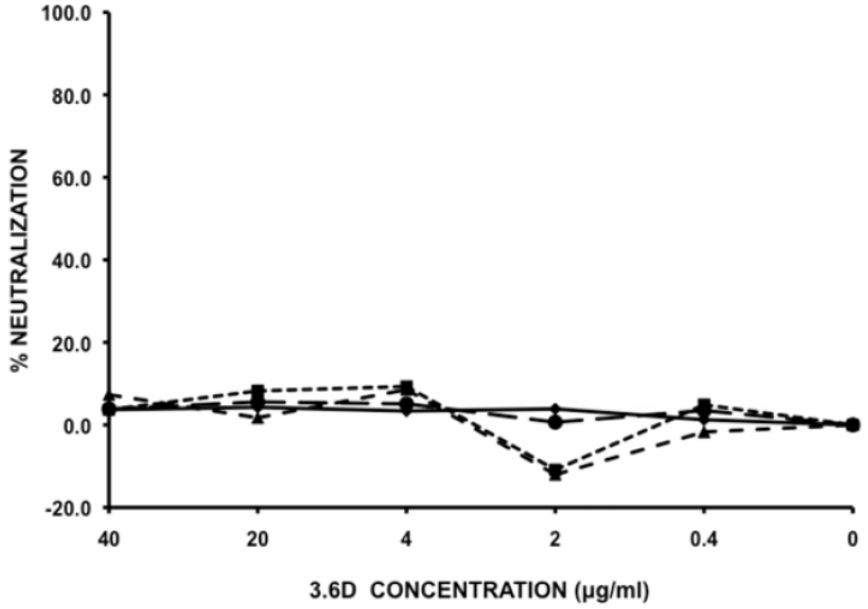

Figure 12: DENV is not neutralized by the 3.6D HMAb.
Approximately 100 FFU of virus were incubated with serial dilutions of purified monoclonal antibody. Virus mixtures were allowed to infect LLC-MK2 cells and then incubated at 37^{o}C. Virus foci were detected using anti-DENV E protein MMAb E60. Results are expressed as pooled data from two independent experiments with three replicates (Schieffelin et al., 2010).

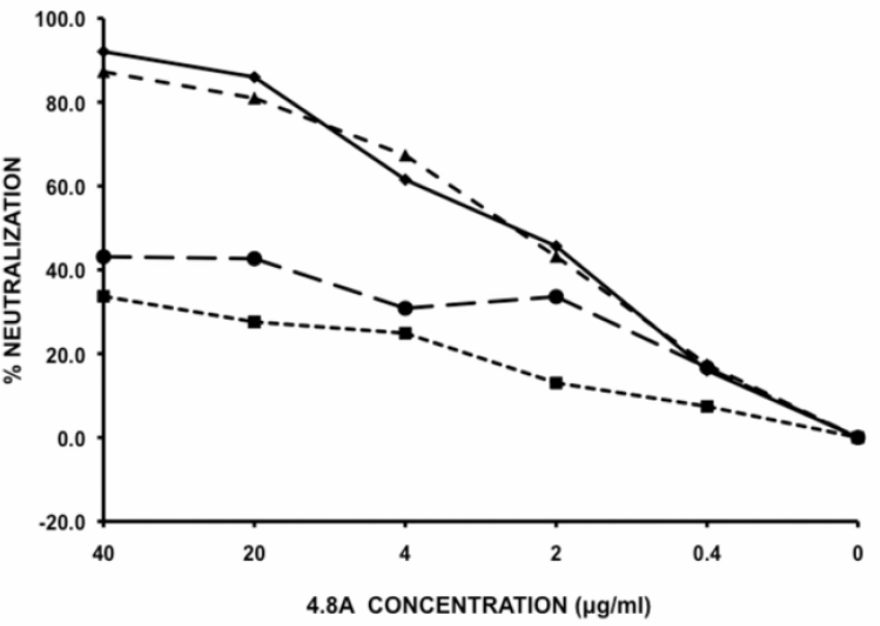

Figure 13: DENV is neutralized by the 4.8A HMAb.
Approximately 100 FFU of virus were incubated with serial dilutions of purified monoclonal antibody. Virus mixtures were allowed to infect LLC-MK2 cells and then incubated at 37^{o}C. Virus foci were detected using anti-DENV E protein MMAb E60. Results are expressed as pooled data from two independent experiments with three replicates (Schieffelin et al., 2010).

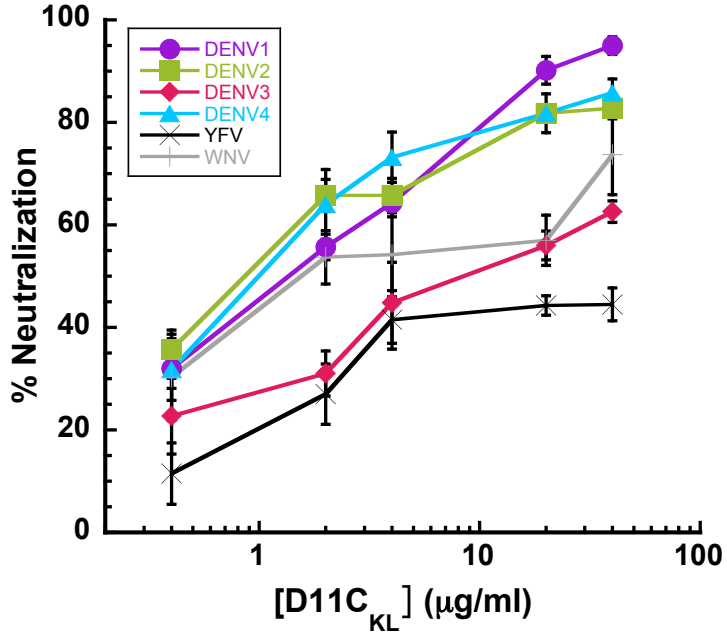

Figure 14: DENV is neutralized by the D11C.KL HMAb.
Approximately 100 FFU of virus were incubated with serial dilutions of purified monoclonal antibody. Virus mixtures were allowed to infect LLC-MK2 cells and then incubated at 37°C. Virus foci were detected using anti-DENV E protein MMAb.

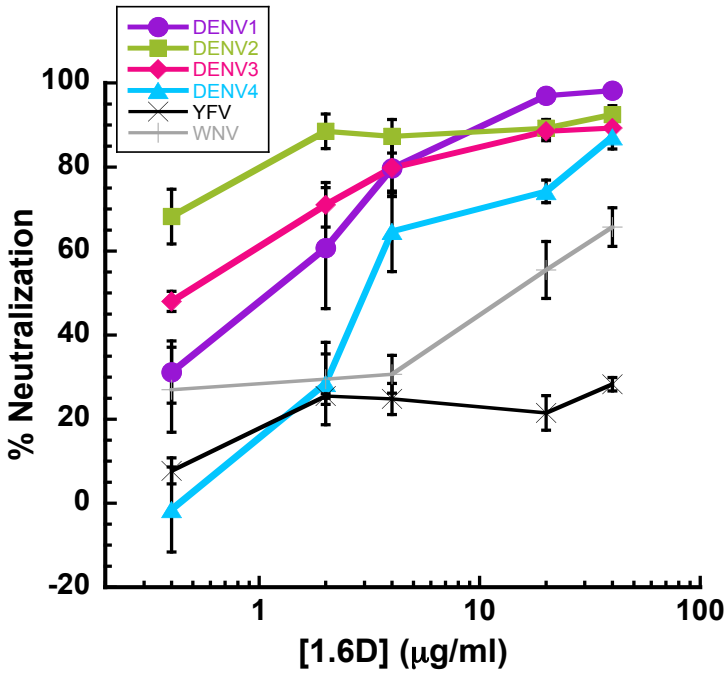

Figure 15: DENV is neutralized by the 1.6D HMAb.
Approximately 100 FFU of virus were incubated with serial dilutions of purified monoclonal antibody. Virus mixtures were allowed to infect LLC-MK2 cells and then incubated at 37°C. Virus foci were detected using anti-DENV E protein MMAb.

4.3 Antibody enhancement of viral entry

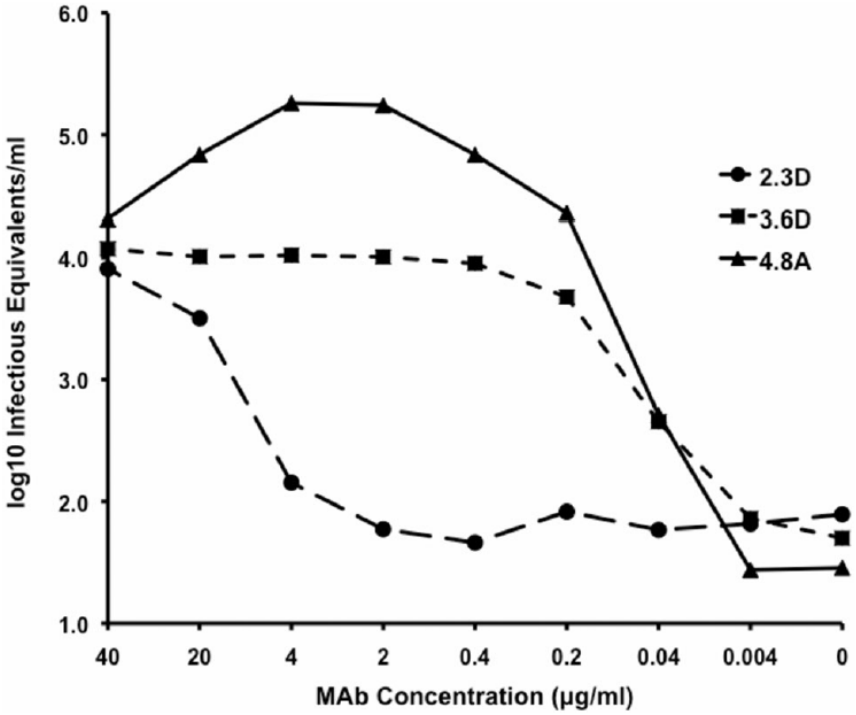

Figure 16: Enhanced DENV infection by K562 cells in the presence of HMAbs.
Fc receptor expressing human K562 cells were infected with DENV-1 in the presence of increasing concentrations of the antibodies. RNA was extracted from cell lysates and quantitative RT-PCR was performed with a DENV-1 specific primer pair specific for the NS1 region as a measure of infectious equivalents (Schieffelin et al., 2010).

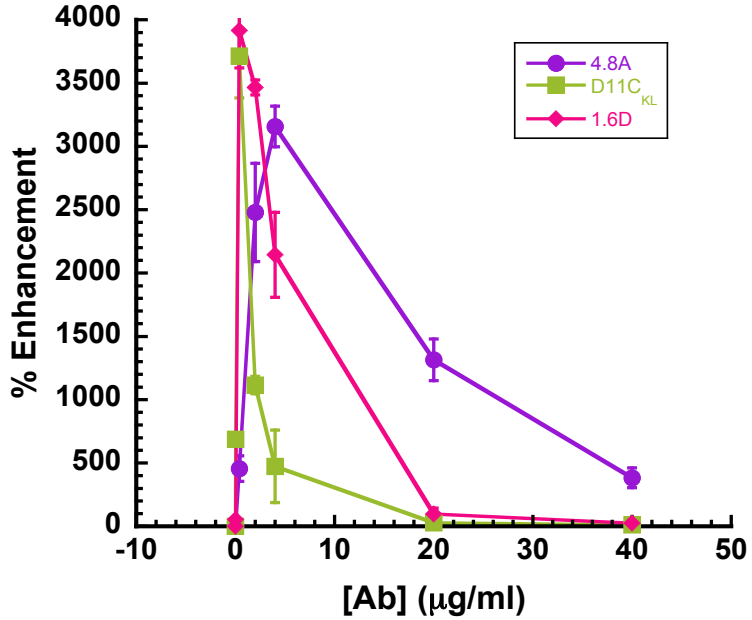

Figure 17: Infection of DENV-1 into K562 cells with 4.8A, D11C.KL, and 1.6D hMAbs.
HMAbs mediate enhancement into Fc receptor bearing cells.

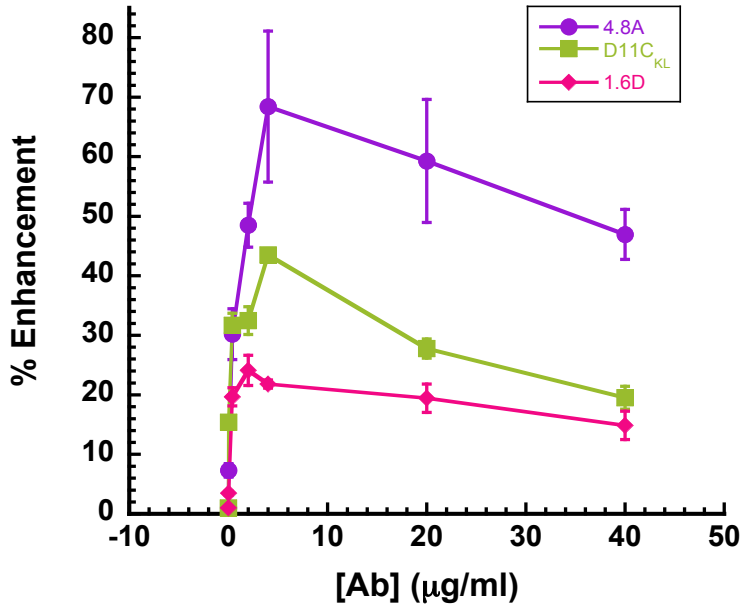

Figure 18: Infection of DENV-2 into K562 cells with 4.8A, D11C.KL, and 1.6D hMAbs. HMAbs mediate enhancement into Fc receptor bearing cells.

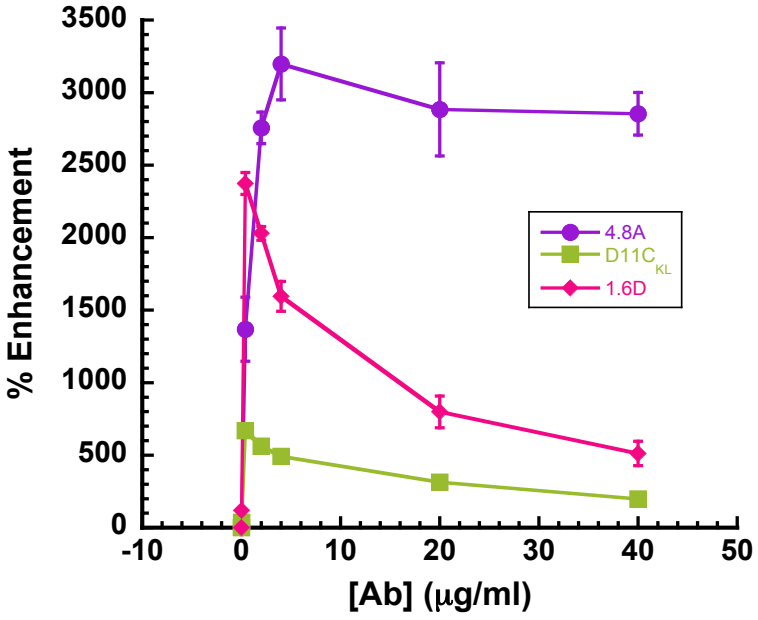

Figure 19: Infection of DENV-3 into K562 cells with 4.8A, D11C.KL, and 1.6D hMAbs. HMAbs mediate enhancement into Fc receptor bearing cells.

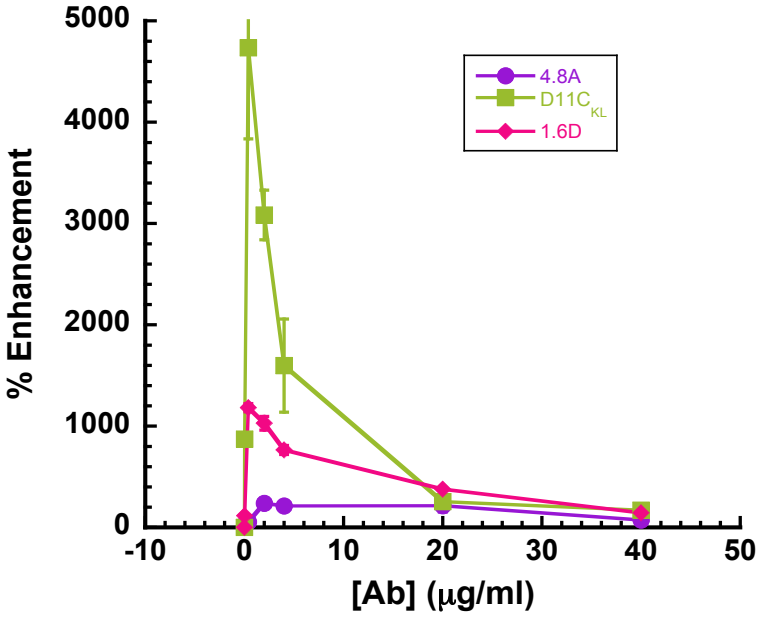

Figure 20: Infection of DENV-4 into K562 cells with 4.8A, D11C.KL, and 1.6D hMAbs. HMAbs mediate enhancement into Fc receptor bearing cells.

4.4 Biolayer interferometry binding studies of HMAbs

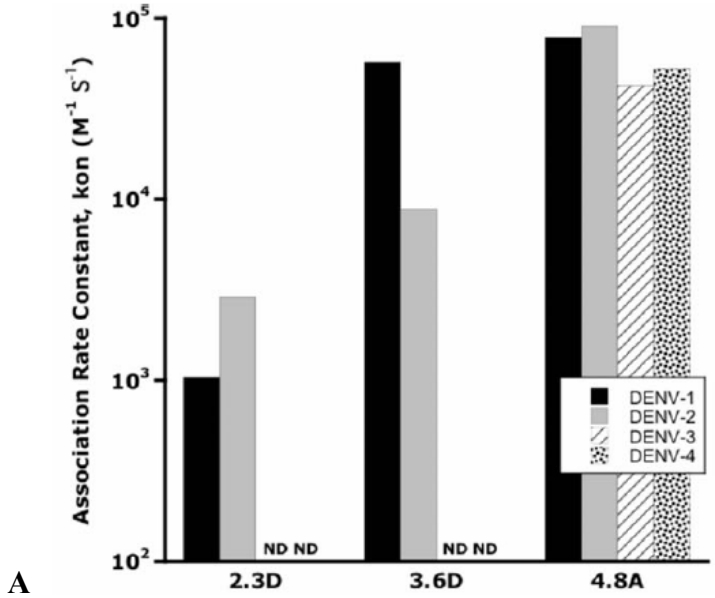

A

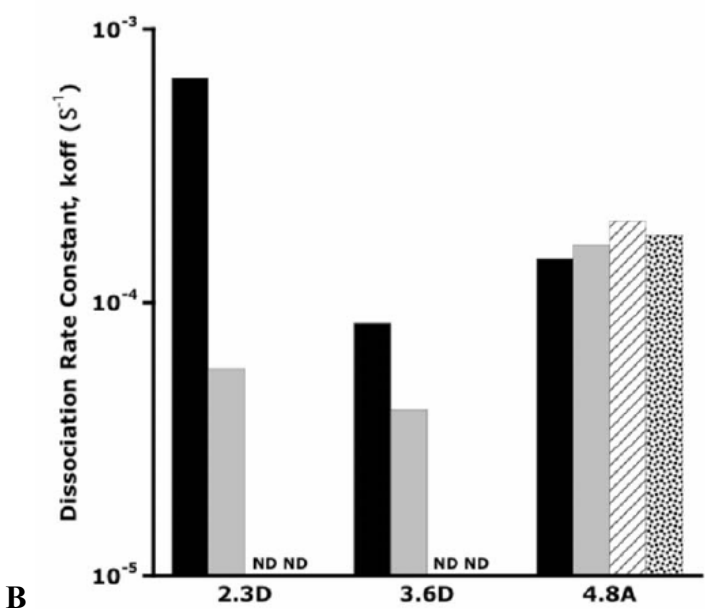

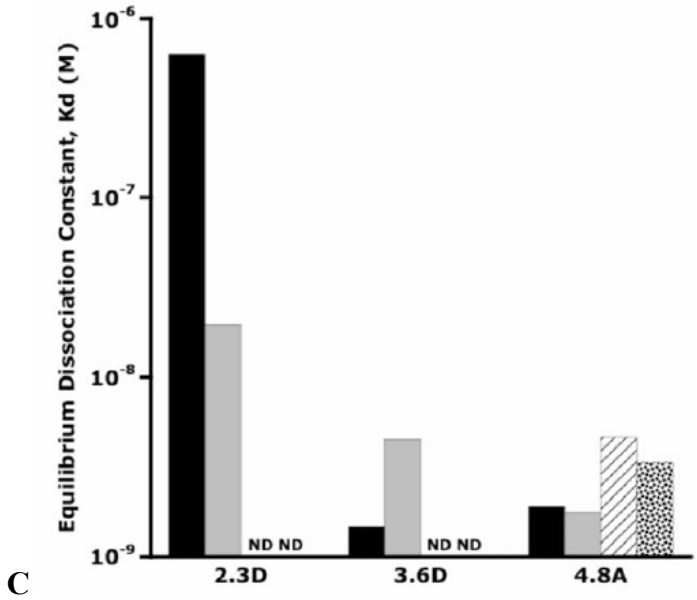

Figure 21: HMAbs 2.3D, 3.6D, 4.8A affinity measured by biolayer interferometry.
Label free, real time binding analysis between the HMAbs 2.3D, 3.6D and 4.8A and purified, recombinant E protein from each DENV serotype to measure binding affinity was performed. The affinities of 2.3D and 3.6D for DENV 3 or 4 E proteins could not be measured due to Ab aggregation at the higher concentrations needed to detect lower affinity binding. A: Association rate constants (kon) for Ab:E protein interactions. B: Dissociation rate constants (koff) for Ab:E protein interactions. C: Equilibrium dissociation constants (K_D) for HMAb:E protein complexes (Schieffelin et al., 2010).

	4.8A	D11C$_{KL}$	1.6D
DENV-1	6.7E-10	4.0E-10	2.8E-10
DENV-2	7.5E-10	1.8E-09	1.9E-09
DENV-3	1.4E-09	3.3E-09	1.8E-09
DENV-4	1.2E-09	4.7E-10	1.6E-09

Table 1: Dissociation constants (K_D) for hMAbs 4.8A, D11C.KL, and 1.6D.

4.5 CryoEM of virus HMAb complexes

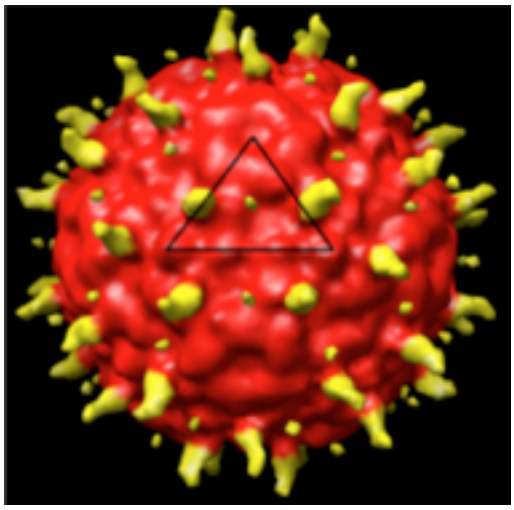

Figure 22: Preliminary cryo-electron microscopy reconstruction of D11C HMAb bound DENV-2 particles.

Conclusions

For the past several decades, the immunological response against DENV has been studied using monoclonal antibodies generated in mice. This is very surprising since mice are not naturally infected, nor do they develop disease when infected with DENV. The mouse antibody response is very different from the human response, and the antibody response in humans is directly linked to disease severity due to ADE. Our group has produced, isolated, and characterized the first human monoclonal antibodies against DENV surface proteins and published the first ever manuscript describing this work (Schieffelin et al., 2010). This work has answered several questions that will be critical for the development of DENV vaccines and antivirals.

Task 5: Liposomal assays determine alkaline flux rates and report on membrane fluidity changes which increase alkaline flux.

Introduction

We have invented a germicide formulation that kills by creating an alkaline flux into the cytoplasm of living cells. In order to determine the basic mechanism of action, and discover better formulas, we screened for alkaline flux rates with a Teflon membrane apparatus, and followed up with a liposome (also known as vesicle) assay that more closely mimics the cytoplasmic membrane and internal compartment of a real pathogen. By measuring changes in intravesicular pH over time, we were able to determine the alkalinization rate enhancement in the presence of membrane fluidizing agents, we used detergents and ethanol to increase membrane fluidity, in the presence of ammonia, which acted as a 'hydroxophore' and transported OH^- ions across the membrane.

Methods, Assumptions, and Procedures

We varied the four major variables in our biocide formulation by changing the magnitude of the pH gradient, concentration of detergent, alcohol, and ammonia. (In a formulation shown in the liposome figure below we used deoxycholate, ethanol, and ammonia concentration at pH 9 external; pH ~6.5 internal). Our experimental approach was to alter one variable, while holding the other three constant and observe the effect on alkaline liposomal gradient collapse. When an alkaline gradient was imposed an inward flux of free neutral ammonia alkalinized the liposome. By modulating the concentration of one component while holding the other three constant the best formulations were screened (those which maximize alkaline flux, and hence predict biocidal lethality).

Small unilamellar vesicles (SUVs) were prepared with egg phosphatidylcholine and 40 mole% cholesterol. A solution containing 50 mM Na_2SO_4 and 10 mM pyranine (fluorescent pH reporter dye) were added to a lipid film deposited onto glass by evaporation of a solvent, at a lipid concentration of 4 mg lipid/ml. A lipid suspension was vortexed then sonicated to form SUVs of limit size (~250 angstroms). Some pyranine is trapped inside the liposomes, and external pyranine must be removed, which was accomplished by using Sephadex G-25 Gel chromatography. The G-25 column physically separates free dye from the liposomes by using the large differential in size between vesicles and dye. The column mobile phase was 50 mM Na_2SO_4. To check for the absence of extravesicular pyranine, a membrane impermeable, fluorescence quencher dye (DPX) was used, a lack of DPX-pyranine quenching indicated that no external dye was present, any preparation showing more than 5% quenching was discarded. In a 96 black well plate, a volume of SUVs was placed into several wells with 50 mM Na_2SO_4, and 25 mg/mL DPX in dH_2O. The excitation at 415 and 460 nm was read on a Tecan Infinite M1000 plate reader (Emission=514 nm). An isosbestic point, method was used to calculate percent quenching: %quenching = (1-(DPX sample/control)*100%. A volume of SUVs containing parenting and 50 mM Na_2SO_4 at pH 6.5 were placed into additional wells of a 96 black well-plate. The external pH was raised to pH 9 with sodium hydroxide the initial 460/415 ratios work 10 obtained, and then measured over time. The intravesicular pH was then calculated, and plotted vs time, revealing the rate of alkalinization under control and experimental conditions.

Results and Discussion

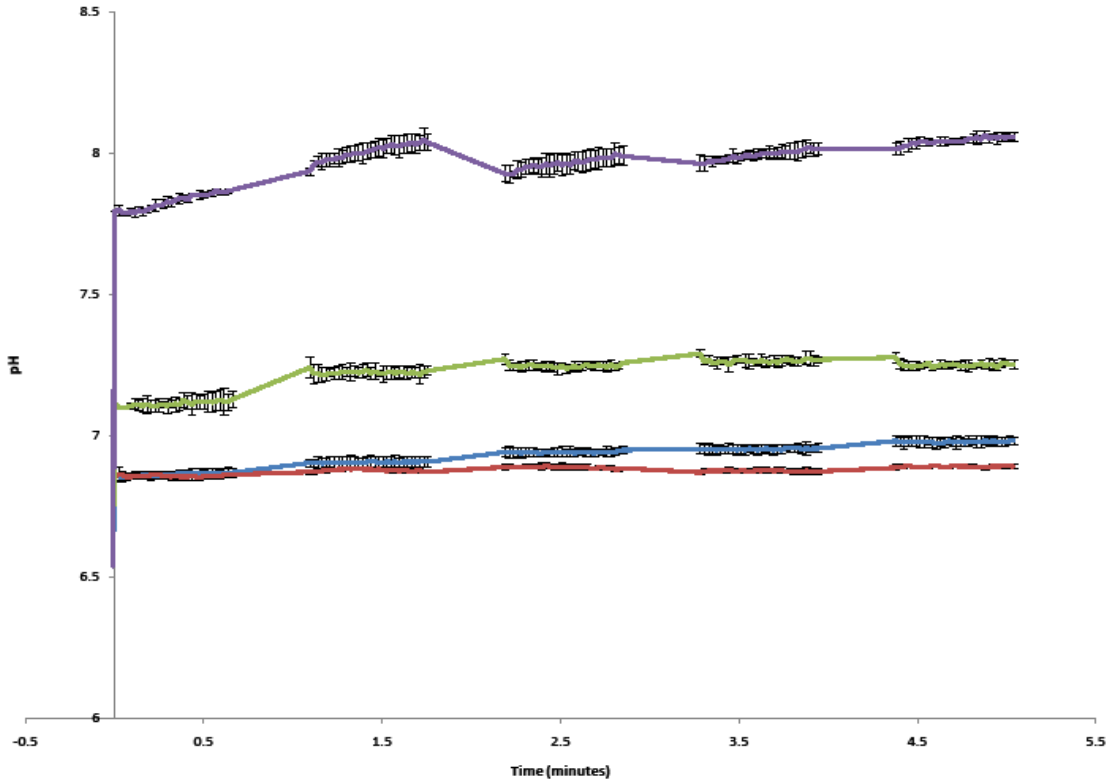

Figure 23. A pH sensitive dye, pyranine, was used to measure the intravesicular pH of SUVs.
A germicide with the following components was formulated: 1% ethanol, red; 1 mM NH_3, blue; 0.5 mM deoxycholate green. The internal pH was 6.5 and the external was pH 9, in each case When these components were combined (purple), the magnitude of the initial pH change greatly increased.

Conclusions

Typically, each component of in our germicide formulation is relatively benign, but the combination was predicted to be lethal to our *Vibrio fischeri* test organism based upon the membrane model work. It is clear from the figure above that all four components are synergistically effective in alkalinizing the interior of a liposome, We speculate that the ethanol and detergent synergistically permeabilized the phospholipid bilayer of the liposome causing an increase in ammonia permeability and that this explains the very large alkalinization rate observed when all four components are present. We chose formulations for germicide that were the most efficacious in creating the collapse of a pH gradient.

Task 6: Chemical assays to determine photocatalytic effectiveness.

6.1 Tartrazine yellow dye photobleaching: A model for investigating the destruction of aqueous targets.

6.2 Sudan red dye photobleaching: A model for investigating the destruction of hydrophobic targets.

Introduction

Certain azo dyes are known to be very resistant to UV light and chemical oxidation. We chose two different UV, photo resistant, hydrophobic and hydrophilic, azo dyes to create a lipoidal and a water soluble model for photocatalytic destruction. All azo dyes contain conjugated pi bond systems $(\sim C=C-C\sim)_n$ and the destruction of any individual C=C double bond in the dye structure will lead to de-colorization of the dye, thus creating a sensitive model for molecular destruction. We tested many photocatalytic formulations with our dye destruction models, including some doped materials produced by metal oxide synthesis (Woodfield et al., 2007).

Methods, Assumptions, and Procedures

Tartrazine yellow was used an 'aqueous target' which would decolorize upon photocatalytic destruction. Sudan red can be encapsulated within the hydrocarbon core of a detergent micelle in order to investigate whether the ROR (radicals, oxidants and reductants) which are generated in water during photocatalysis, can destroy a hydrophobic molecule ensconced within a lipid environment (Coates et al., 2007). Notably, the model can also be used for investigating hydrophobic molecular destruction using any ROR source including, gamma irradiation, Fenton reactions, hypochlorite or other chemical systems. We used cetyl trimethylammonium bromide (CTAB), to form the micelles. This particular detergent has a 16 carbon chain with an onium head group. The onium head group is composed of three methyl groups bonded to nitrogen with the chain forming the fourth carbon bond. Our initial choice of detergent leads to a micelle with a maximum diameter of 32 carbons, containing completely saturated carbon chains within the hydrocarbon core, and with a positive charge on the face of the membrane. Unsaturated and poly-unsaturated chains will alter the composition of the micelle and allow mimicry of the lipid environment and surface charge of any bio-membrane. Our model is therefore very flexible in the context of chemical environment, different chain lengths and different head groups, and can lead to many other options for the composition of the micelles, so that mimicry of the lipid environment of any bio membrane is possible.

Unlike sudan red, tartrazine yellow was freely soluble in water, and was used to test the hypothesis that water soluble ROR (in our case from photocatalysis), could destroy the C=C bonds in hydrophilic molecules. Similar to our Sudan model, our aqueous tartrazine dye destruction model can also be used to report on hydrophilic molecule destruction from any ROR source.

Results and Discussion

Tartrazine yellow was a very useful aqueous target to demonstrate photocatalytic effectiveness in all cases we saw photocatalytic bleaching of the yellow color, and we were able to use the rate of bleaching as an index a photocatalytic effectiveness. In some experiments tartrazine adsorbed onto the photocatalytic powder, thus coloring the powder yellow. We recognized that this binding constituted an important advantage. In such a case the photocatalytic powder is capable of removing an aqueous analyte from solution, and destroying it on the face of the powder. Since the powder turned white upon prolonged illumination it is clear that removal and destruction of aqueous toxin is possible with our photocatalytic systems.

More interesting results were obtained with Sudan red Sudan red dye photobleaching, as

shown below. Synthesized TiO2 materials, our patented titanium foil coating (Barreto, 2011), and a commercially available photocatalyst (Evonik P-25) were all used to destroy sudan red, one example using P-25 is shown below:

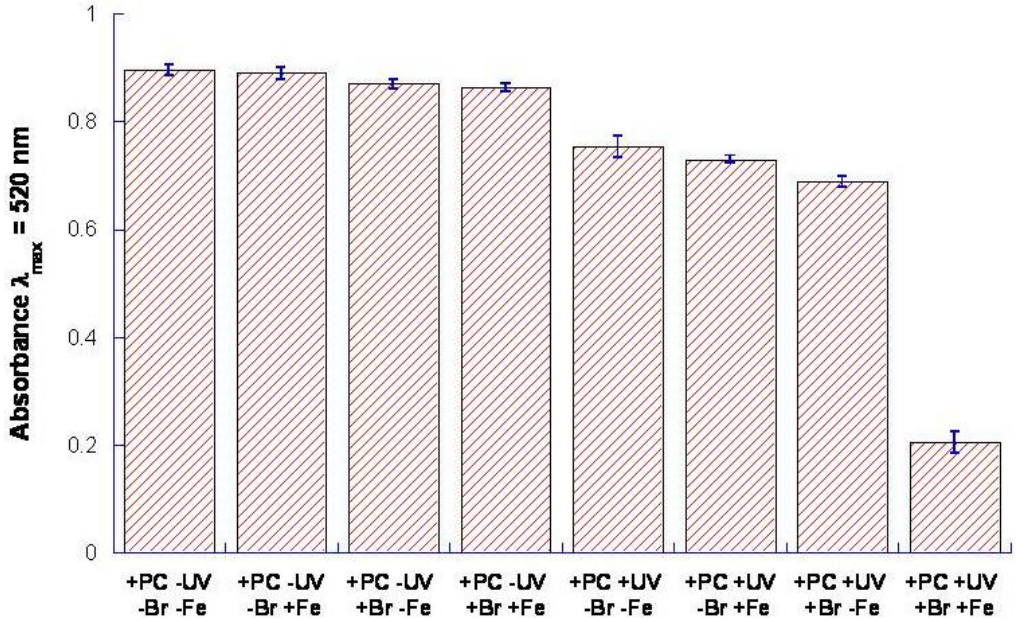

Figure 24. Sudan red in a 100 mM CTAC solution is exposed to P25 TiO_2 coated discs with and without the addition of 221 uM $Fe(NO_3)_3$, 88 mM NaBr and/or 365 nm UV light. Addition of 365 nm UV light without Fe or Br or with Fe or Br separately resulted in an approximately 20% decrease in Sudan red absorbance (Sudan red dye destruction). Addition of 365 nm UV light with both Fe and Br resulted in an approximately 80% decrease in Sudan red absorbance (Sudan red dye destruction).

Legend:
+PC: 12 mm glass coated disk, covered with a commercial photocatalyst
-PC: 12 mm glass coated disk, with no photocatalyst
+UV: Irradiated with long wave UV light
-UV: no irradiation
+Fe: Addition of 221 micro-molar ferric chloride
-Fe: No ferric ion added
+Br: Solution contained 88 millimolar sodium bromide
-Br: No bromide added

Sudan red encapsulated in a CTAC micelle was unaffected by the presence of a photocatalyst with or without ferric and/or bromide ions (four left-hand columns). In the presence of 365 nm UV light, micellar Sudan red was slightly destroyed in the presence of a photocatalyst with or without ferric and/or bromide ions (next three columns). Micellar Sudan red was mostly destroyed in the presence of UV light, photocatalyst, ferric ion and bromide ion (right-hand column).

The CTAB detergent we used to encapsulate sudan red is lipophilic target that used a bromide counter ion, so that these detergent solutions contain 100mM Br^-. Very recently we became aware of work showing that a solution of sodium bromide (NaBr) can generate the tri-bromide anion (Br_3^-) upon irradiation with gamma rays, via a series of reactions that involve

bromine radicals and various oxy-bromide intermediate species. Br_3^- is a stable final product that can also be generated via a reaction between Br^- and Br_2, we chemically synthesized Br_3^- with this reaction and recorded the shape and maximum (266nm) of the resultant absorbance spectrum. We now report photocatalytic generation of the tri-bromide anion, the wavelength of maximum absorbance and shape of the curve exactly match the spectrum of Br_3^- . The spectrum is also identical the spectrum published in a recent manuscript where gamma rays were the source of bromine radicals from sodium bromide. Our recent discovery is evidence that a photocatalytic decontamination system can generate products identical to gamma irradiation, it sheds much light on the mechanism of photocatalysis and indicates that decontamination with both types of radiation utilizes a similar mechanism.

To 18 mls of 4M NaBr solution were added 1.0 mg/ml of P25 TiO_2 suspended in water. A UVP Pen Ray 365 nm lamp previously warmed for 3 minutes was placed into the solution with stirring. At one-minute time points, a 500 µl sample was removed from the solution and replaced with an equal volume of fresh solution. The samples were microfuged to remove the P25 TiO_2 powder. 300 µl of each sample was placed into a semi-micro quartz cuvette and scanned on a Shimadzu UV-2450 spectrophotometer.

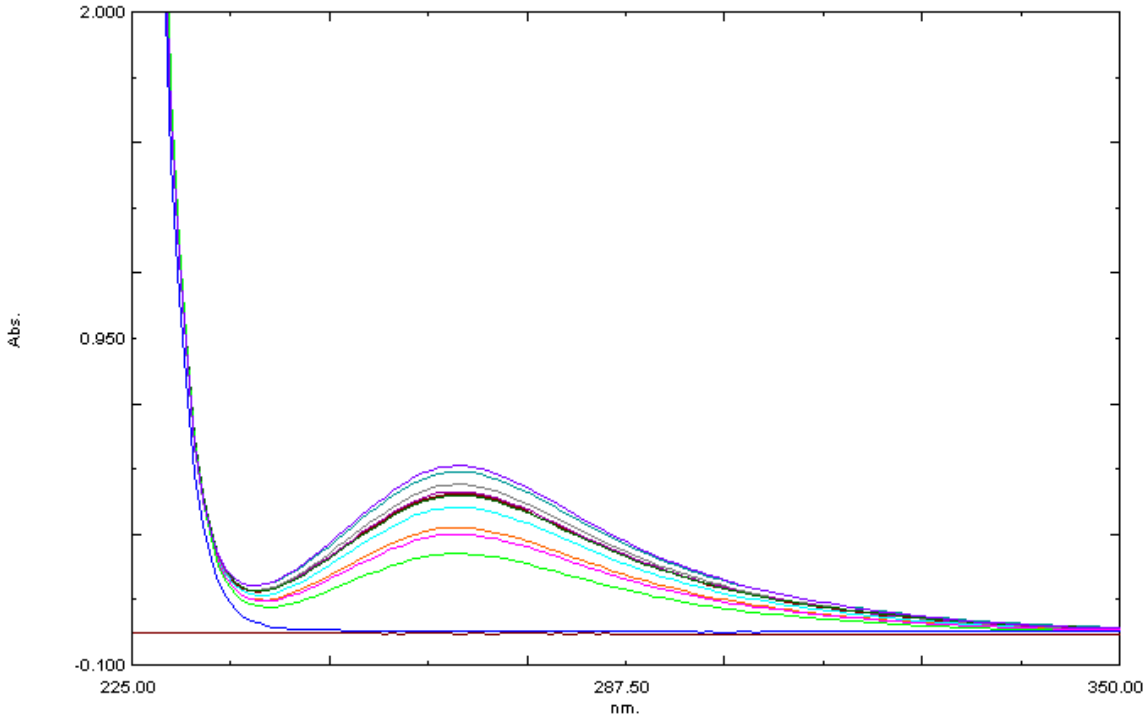

Figure 25. The UV scan shows the result of 10 consecutive 1-minute intervals of illumination of 4M NaBr, with 365nm UV light, in the presence of an Evonik P-25 TiO_2 photocatalyst.
More product appears with each interval, the absorbance peak is at 266nm.

Conclusions

During aqueous tartrazine destruction experiments it became clear that (1) Removal and destruction of aqueous toxin is possible with our photocatalytic systems, since our photocatalytic powders were colored yellow by the tartrazine dye but both the powder and solution became colorless during photocatalytic destruction (2) The combination of bromide and ferric ion

produces very large enhancements of destruction for a lipophilic target (sudan red IV). The system holds great promise for the destruction of targets sequestered in the hydrocarbon core of a cell membrane, destruction of membrane components leads to lethality so this system is capable of destroying lipophilic toxins and holds promise as a germicide for living cells. We have discovered that the addition of small amounts of bromide and iron to the photocatalytic system composed of TiO_2 greatly enhances the destruction of a lipohilic dye target, implying great efficacy for the destruction of targets inside the hydrocarbon core of a cell plasma membrane. It is well known that hydroxyl radicals are generated by gamma rays, and we have used a terephthalate dosimeter to measure gamma rays and more recently, photocatalytic effectiveness, (Barreto et al., 1995). (3) The presence of bromide during photocatalysis produced Br_3^- a second chemical species that produced by gamma ray irradiation and photocatalysis.

Task 7: Screening with Vibrio fischeri for killing effectiveness with alkaline biocides and photocatalysts.

Introduction

Our biocide formulations were designed to be convenient, inexpensive and safe, they use relatively non-toxic individual components which are stable indefinitely in aqueous solution, and can be stored separately before use. When the individual components are mixed together, the combination becomes extremely lethal to all pathogens. After use, when deployed as a spray on contaminated surfaces, the volatile components (ammonia and ethanol) evaporate, and the germicidal lethality is 'switched off' leaving behind little or no residual toxicity. The mechanism of killing is the elevation of cytoplasmic pH. We can create an inwardly directed flux of hydroxide ions by using a high external pH, and add components (detergent and ethanol) which serve to permeabilize the cell plasma membranes. The alkaline flux raises the cytoplasmic pH of living cells past the point of viability; the mechanism of killing is generic, a sufficiently high internal pH will kill any living cell.

Methods, Assumptions, and Procedures

Herein, we extend, and confirm our previously reported work, which used abolition of *Vibrio fischeri* as a model for germicidal effectiveness. Notably these luminescent marine vibrios are extremely hardy to ammonia and high pH making them a 'hard target' for the testing of our alkaline biocides. Each germicidal formula below has been coded with a Roman numeral and listed in the Table, below. CTAC (16C), and TTAC (14C) are quaternary ammonium detergents of varying carbon chain length, the other components are ammonia, an alcohol, and a pH elevated to pH 9, (or higher with NaOH).

Table 2: Biocide formulas.

Biocide	Components	100 mM Detergent	99.9% Alcohol	1 M NH3	dH2O	pH
I	5 mM CTAC, 5% Ethanol, 5 mM NH3, NaOH	2.5 mL	2.5 mL	250 uL	44.75 mL	Solid NaOH pH 9
II	5 mM CTAC, 5% Isopropanol, 5 mM NH3, NaOH	2.5 mL	2.5 mL	250 uL	44.75 mL	Solid NaOH pH 9
III	5 mM TTAC, 5% Ethanol, 5 mM	2.5 mL	2.5 mL	250 uL	44.75 mL	Solid NaOH pH 9

	NH3, NaOH					
IV	10 mM TTAC, 10% Isopropanol, 10 mM NH3, NaOH	5 mL	5 mL	500 uL	39.50 mL	Solid NaOH pH 9
V	5 mM TTAC, 5% Isopropanol, 5 mM NH3, NaOH	2.5 mL	2.5 mL	250 uL	44.75 mL	Solid NaOH pH 9
VI	2.5 mM TTAC, 2.5% Isopropanol, 2.5 mM NH3, NaOH	1.25 mL	1.25 mL	125 uL	47.38 mL	Solid NaOH pH 9
VII	1.25 mM TTAC, 1.25% Isopropanol, 1.25 mM NH3, NaOH	625 uL	625 uL	62.5 uL	48.69 mL	Solid NaOH pH 9
VIII	15 mM NH3, NaOH	-	-	750 uL	49.25 mL	Solid NaOH pH 9
IX	5 mM NH3, NaOH	-	-	250 uL	49.75 mL	Solid NaOH pH 9

a) Culturing *Vibrio*: *Vibrio fischeri* was initially cultured by adding ~10 mg lyophilized bacteria to 50 mL filter-sterilized photobacteria broth (PBB) in a large culture flask using sterile techniques. Cultures were incubated at 25°C and rotated gently (36 RPM). Every day a subculture was prepared from the previous day's culture by diluting 200 uL of 24-hour old *Vibrio* to 10 mL with sterile PBB.

b) Preparing Daily Stock *Vibrio*: Immediately before toxicity was tested, a 24-hour old *Vibrio* culture was diluted in PBB so that the initial RLU measurement of a control sample in the well plate is 500,000 units. This improves our ability to compare data from day to day and guarantees that the *Vibrio* will not become too luminescent during their normal growth for the luminometer.

c) Testing Biocide Toxicity: In a clear 24-well plate, 100 uL of each biocide formula was added to 300 uL aliquots of daily stock *Vibrio*. As a negative toxicity control, deionized H_2O was added in place of biocide. The well plate was placed on a rotator set to high speed for 30 seconds to mix the contents. Total treatment time was five minutes. After five minutes, 28.6 uL was transferred in triplicate from each well of the 24-well plate to a white 96-well plate, where it was diluted in 171 uL PBB (total volume 200 uL). Three wells containing 200 uL sterile PBB were added as a negative luminescence control through which luminescent crosstalk or well-to-well contamination could be identified. *Vibrio* luminescence was monitored once an hour for >24 hours using a Tecan M1000.

Results and Discussion

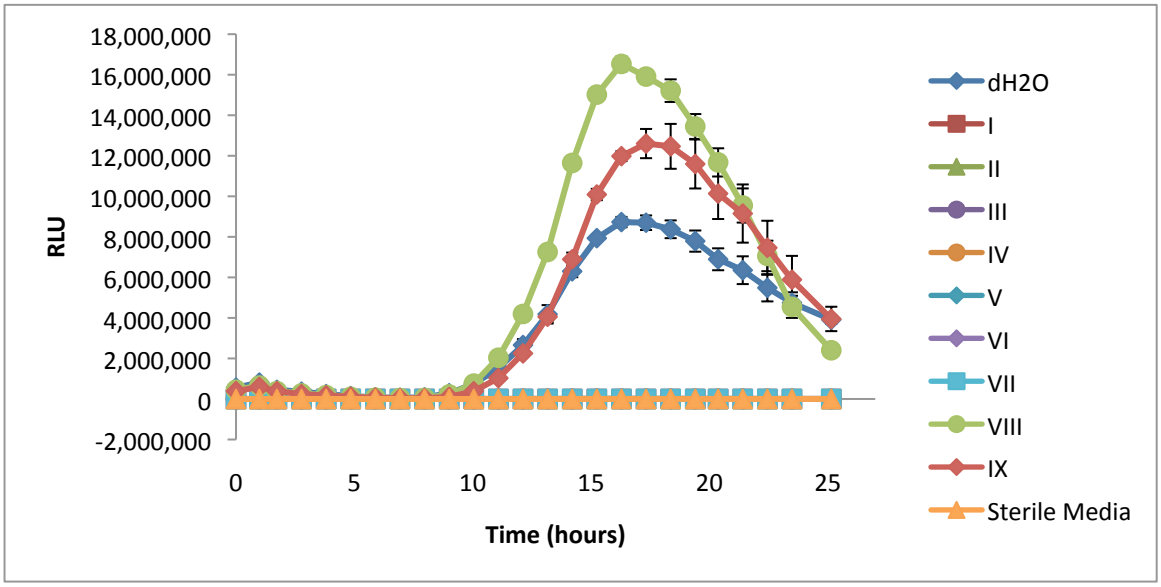

Figure 26. The relative luminescence values of *Vibrio*.
High RLU values denote active metabolism and growth, lower RLU values signify injury, death is indicated by zero RLU values which do not rise. We treated the vibrios for 5 minutes with each germicidal solution followed by a 25-hour re-growth period. Growth curves show a peak of luminescence (RLU) at approximately 16 hours of growth in a well plate.

A de-ionized water control, (dark blue diamonds), showed diminished growth, which we attribute to osmotic shock, since our marine *vibrios* prefer a hyper-saline environment. . Ammonia controls constituted treatments VIII (15mmM) and IX (5mM) which were adjusted to pH >9.0 Interestingly, marine vibrios grew best in the 15 mM NH_3 (green circles) and 5 mM NH_3 (red diamonds) alkaline media treatments, showing that these vibrios are alkaline extremeophiles that thrive in a high pH environment, even in the presence of a permeable base like ammonia. Most notably, germicides which included I-VII, and contained a quaternary detergent, alcohol and ammonia, (the complete biocide formulation) were all extremely lethal. At pH 9 the biocide growth curves for I-VII cannot be seen because the luminescence never develops and the values run close to background, zero RLU, (along the x-axis). Note that the I-VII results are identical to our negative control, sterile media in which no *Vibrio* were added.

Conclusions

As expected, the luminescent marine vibrios proved to be difficult targets to kill with an alkaline germicide they constitute an alkaline hardy organism, even high pH and ammonia did not kill the luminescent vibrios, indeed some cultures flourished with such a treatment. When a detergent, alcohol, ammonia and high pH were combined the vibrios succumbed to the germicidal treatment.

Task 8: Biocidal testing with model pathogens.

Introduction

In screening tests *Vibrio fischeri* was killed by all of our complete biocide formulas (I through VII above). Because our testing measured luminescence, a metabolism-linked process we showed that the combined formulas were lethal even at dilute concentrations (see biocide VII). Further testing with pathogens was conducted to reveal the efficacy of our biocides against other bacterial strains. Based upon Dr. Barreto's previously reported Vibrio work, using abolition of vibrio fischeri as a model for biocidal effectiveness (see above) we proceeded with the ' best candidate' alkaline biocide formulas for final testing with an independent contractor, (as described in our original proposal) the best candidates were tested by Dr. Joseph Lepo at the University of West Florida, all samples were coded so that the testing lab was not aware of the composition of the solutions before testing.

Methods, Assumptions, and Procedures

We chose *Mycobacterium smegmatis*, *Alcaligenes faecalis*, *Escherichia coli*, *Staphylococcus aureus*, *Bacillus cereus* and *Pseudomonas aeruginosa as a panel for systematic testing of germicidal effectiveness.* Inhibition of re-growth (measured as an absence of turbidity in the media; also via colony counts on agar plates) was used as an index of germicidal efficacy.

a) Bacterial cultures were grown in broth media for 24 hours before testing began.
   i. *V. fischeri* was grown in PBB
   ii. *M. smegmatis* was grown in Nutrient Broth
   iii. *A. faecalis, P. aeruginosa, B. cereus, E. coli,* and *S. aureus* were grown in Full Strength Tryptic Soy Broth
b) The optical density (O.D.; absorbance at 450 nm) of each culture was checked after the 24 hour growth period and adjusted to an O.D. of 1.0, if needed.
c) From adjusted bacterial cultures, 500 uL aliquots were treated for five minutes in sterile 24-well plates with 500 uL of the biocide formulas.
d) After the 5 min incubation, the entire 1 mL volume was transferred from individual wells of the 24-well plate into sterile culture tubes pre-filled with 6 mL of the appropriate media.
e) The culture tubes were shaken to homogenize and then 0.5 mL was removed to record O.D. of each culture tube.
f) 100 µL was removed from each culture tube to make a serial dilution series for plate counts. For the first run with each organism, the following dilutions were made: 10^{-2}, 10^{-4}, 10^{-6}, 10^{-8}, 10^{-10}. In replicate experiments, only the dilutions needed to achieve a countable plate were prepared.
g) 100 µL of each dilution was aliquoted onto the appropriate plate and spread using a flame-sterilized spreader.
h) Inoculated plates were placed in the incubator.
i) After 24 hours of growth, the plates were removed from the incubator and colony counts performed.
j) Culture tubes were placed in the shaking incubator until the remaining sample times (24 hours and 96 hours), when steps d through h were repeated.

Results and Discussion

We systematically tested all biocides against all organisms and report herein the most important results. Most of the biocides we formulated were very effective germicides, we discovered one very hardy and difficult to kill bacterium, namely, *Pseudomonas aeruginosa* with our screening panels.

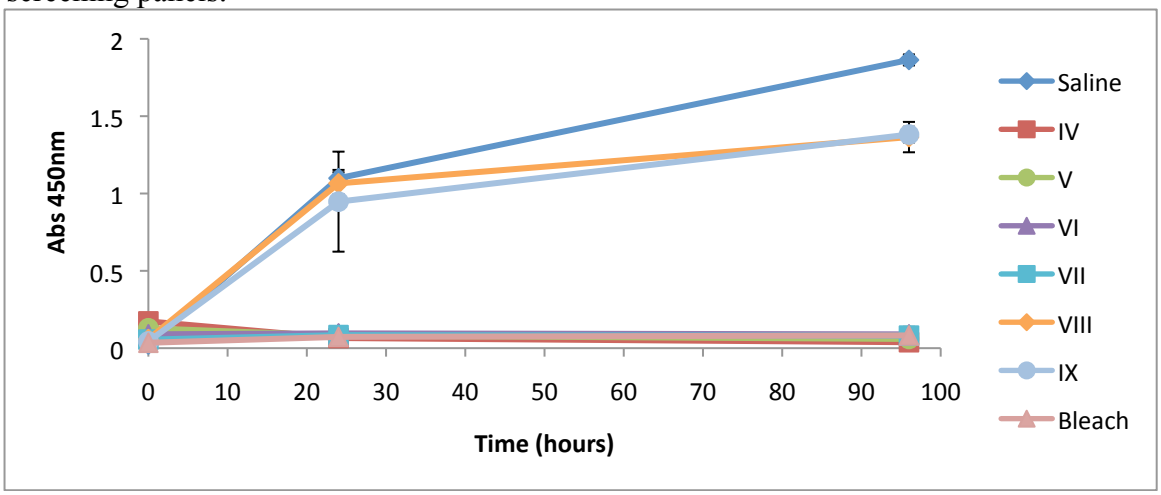

Figure 27. As bacterial cultures grow the increased number of organisms in solution creates turbidity due to light scattering.
The turbidity can be quantified by measuring the optical density of the liquid cultures at 450 nm, the scattered light is interpreted by any standard optical spectrophotometer as an absorbance wherein Absorbance = -log [Transmittance]; Absorbance is also referred to as optical density, OD. On the y-axis above; an increasing absorbance at 450nm means increasing turbidity and growth of *Pseudomonas aeruginosa.* Killing is shown by an absorbance which fails to increase from background and remains close to zero.

Saline was used as a negative toxicity control and bleach as a positive lethal control. Formulas IV through VII differed only in concentration from each other, and were all lethal to *P. aeruginosa*, observed above as very low optical densities and (in separate experiments), as a lack of colony formation on agar plates. Formulas VIII and IX contained only ammonium hydroxide (15 mM and 5 mM, respectively) which raised to pH >9.0; these treatments resulted in regrowth and reveal *P. aeruginosa*'s hardiness to ammonia and alkalinity. We conclude that, *P. aeruginosa* is a hard target and is similar to *Vibrio fischeri* as an alkaline hardy organism which needs the other components for complete killing. Other bacteria in the panel were less hardy *P. aeruginosa*, and were killed by all the alkaline biocides.

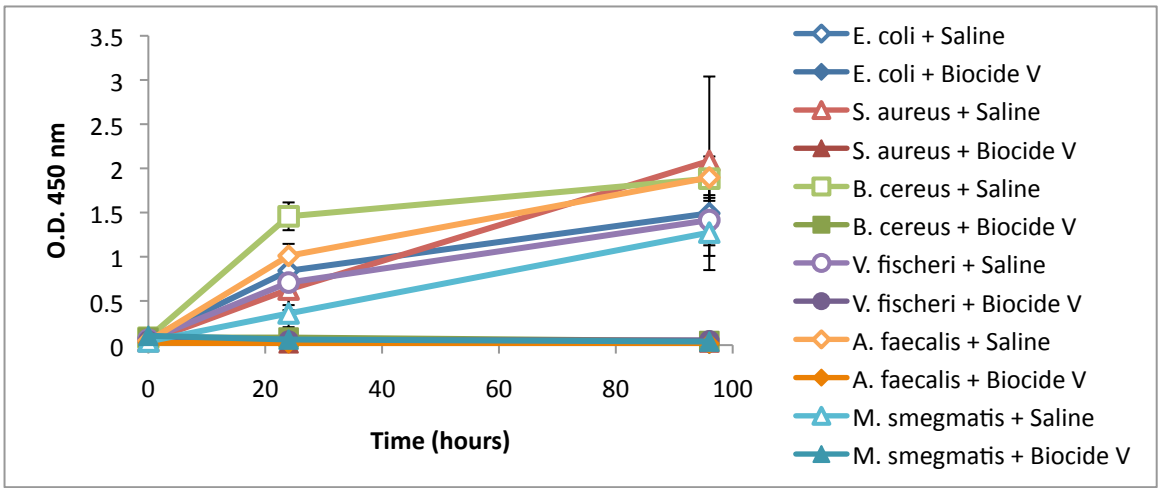

Figure 28. An absorbance (OD) increase indicates growth.
A zero OD change indicates killing (See *Pseudomonas aeruginosa)* legend above.

Our data shows that normal growth curve occurred with the six different bacterial species treated with a saline control solution (open markers). Here we show sample data with biocide V. A complete lack of growth is observed when the cultures have been exposed to a brief five min treatment with Biocide V (filled markers). Re-growth is a very stringent test of lethality since even a few bacteria remaining alive after the five min treatment can re-populate the solution and restore turbidity (OD) to high levels. This was confirmed with colony count experiments on agar plates; no colonies were counted for any of the treated bacteria.

Conclusions

All seven of the bacterial species tested were killed by our complete biocide formula including V. *P. aeruginosa,* which was killed even by biocide VII (a 25% dilution of formula V). In contrast, *P. aeruginosa*'s hardiness to 15 mM alkaline ammonia (biocide VIII) proves that although individual components at high concentrations may be non-lethal, our combined formula is lethal even when dilute.

References

Balcerzyk A, LaVerne J, Mostafavi M. "Direct and Indirect Radiolytic Effects in Highly Concentrated Aqueous Solutions of Bromide". *Journal of Physical Chemistry* 115:4326-4333 (2011).

Barreto JC, Smith GS, Strobel NH, McQuillin PA, Miller TA. "Terephthalic acid: a dosimeter for the detection of hydroxyl radicals in vitro". *Life Sciences* 56(4):PL89-PL96 (1995).

Barreto JC. "Methods for producing photocatalytic material and apparatus therewith. US Patent application serial number: 12/994,215 Published (2011).

Barreto JC. "Antimicrobial composition and methods and apparatus for use thereof. US Patent application serial number: 12/833,510, Published (2011).

Bower MJ, Cohen FE, Dunbrack RL, Jr. "Prediction of protein side-chain rotamers from a backbone-dependent rotamer library: a new homology modeling tool". *Journal of Molecular Biology* 267:1268-1282 (1997).

Chutinimitkul S, Payungporn S, Theamboonlers A, Poovorawan Y. "Dengue typing assay based on real-time PCR using SYBR Green I". *Journal of Virological Methods* 129: 8-15 (2005).

Coates CM, Caldwell W, Alberte RS, Barreto PD, Barreto JC. "Beta-carotene protects sudan (IV) from photocatalytic oxidation in a micellar model system: Insight into the antioxidant properties of the golden staphylococcus aureus". *World Journal of Microbiology and Biotechnology* 23:1305-1310 (2007).

Costin JM, Jenwitheesuk E, Lok S-M, Hunsperger E, Conrads KA, Fontaine KA, Rees CR, Rossmann MG, Isern S, Samudrala R, Michael SF. "Structural optimization and de novo design of dengue virus entry inhibitory peptides". *PLoS Neglected Tropical Diseases* 4(6): e721 doi: 10.1371/journal.pntd.0000721 (2010).

Cuzzubbo AJ, Endy TP, Nisalak A, Kalayanarooj S, Vaughn DW, Ogata SA, Clements DE, Devine PL. "Use of recombinant envelope proteins for serological diagnosis of dengue virus infection in an immunochromatographic assay". *Clinical and Diagnostic Laboratory Immunology* 8(6):1150-1155 (2001).

Finn ST, Strnad JA, Barreto PD, Fox ME, Torres J, Sweeney JD, Barreto JC. "A screening technique useful for testing the effectiveness of novel 'self-cleaning' photocatalytic surfaces". *Photochemistry and Photobiology* in press (2011).

Halstead SB. "Neutralization and antibody-dependent enhancement of dengue viruses". *Advances in Virus Research* 60:421-467 (2003).

Henchal EA, McCown JM, Burke DS, Seguin MC, Brandt WE. "Epitopic analysis of antigenic determinants on the surface of dengue-2 virions using monoclonal antibodies". *American Journal of Tropical Medicine and Hygiene* 34(1):162-169 (1985).

Hrobowski YM, Garry RF, Michael SF. "Peptide inhibitors of dengue virus and West Nile virus infectivity". *Virology Journal* 2:49 (2005).

Huang E, Samudrala R, Park B. "Scoring functions for ab initio folding". In: Walker J WD, ed. *Predicting Protein Structure: Methods and Protocols*: Humana Press (2000).

Levitt M. "Energy refinement of hen egg-white lysozyme". *Journal of Molecular Biology* 82:393-420 (1974).

Levitt M. "Molecular dynamics of native protein. I. Computer simulation of trajectories". *Journal of Molecular Biology* 168:595-617 (1983).

Levitt M, Lifson S. "Refinement of protein conformations using a macromolecular energy minimization procedure". *Journal of Molecular Biology* 46:269-279 (1969).

Metropolis N, Rosenbluth AW, Rosenbluth MN, Teller AH, Teller E. "Equation of state calculations by fast computing machine". *Journal of Chemical Physics* 21:1087-1092 (1953).

Modis Y, Ogata S, Clements D, Harrison SC. "A ligand-binding pocket in the dengue virus envelope glycoprotein". *Proceedings of the National Academy of Science USA* 100:6986-6991 (2003).

Morita K, Tanaka M, Igarashi A. "Rapid identification of dengue virus serotypes by using polymerase chain reaction". *Journal of Clinical Microbiology* 29(10):2107-2110 (1991).

Nicholson CO, Costin JM, Rowe DK, Lin L, Jenwitheesuk E, Samudrala R, Isern S, Michael SF. "Viral entry inhibitors block dengue antibody-dependent enhancement in vitro", *Antiviral Research* 2011 89:71–74 (2011).

Rees CR, Costin JM, Fink RC, McMichael MM, Fontaine KA, Isern S, Michael SF. "In vitro inhibition of dengue virus entry by p-sulfoxy-cinnamic acid and structurally related combinatorial chemistries". *Antiviral Research* 80:135-142 (2008).

Robinson JE, Holton D, Liu J, McMurdo H, Murciano A, Gohd R. "A novel enzyme-linked immunosorbent assay (ELISA) for the detection of antibodies to HIV-1 envelope glycoproteins based on immobilization of viral glycoproteins in microtiter wells coated with concanavalin A". *Journal of Immunological Methods* 132(1):63-71 (1990).

Robinson JE, Holton D, Pacheco-Morell S, Liu J, McMurdo H. "Identification of conserved and variant epitopes of human immunodeficiency virus type 1 (HIV-1) gp120 by human

monoclonal antibodies produced by EBV-transformed cell lines". *AIDS Research and Human Retroviruses* 6(5):567-579 (1990).

Samudrala R, Moult J. "An all-atom distance-dependent conditional probability discriminatory function for protein structure prediction". *Journal of Molecular Biology* 275:895-916 (1998).

Schieffelin JS, Costin JM, Nicholson CO, Orgeron NM, Fontaine KA, Isern, S, Michael SF, Robinson JE. "Neutralizing and non-neutralizing monoclonal antibodies against dengue virus E protein derived from a naturally infected patient". *Virology Journal* 7:28 (2010).

Thaisomboonsuk BK, Clayson ET, Pantuwatana S, Vaughn DW, Endy TP. "Characterization of dengue-2 virus binding to surfaces of mammalian and insect cells". *American Journal of Tropical Medicine and Hygiene* 72: 375-383 (2005).

Woodfield, BF, Shengfeng L, Juliana BG, Qingyuan L. "Preparation of uniform nanoparticles of ultra-high purity metal oxides, mixed metal oxides, metals, and metal alloys". Patent # CODEN: PIXXD2 WO2007098111 A2 20070830 (2007).

Xiang SH, Doka N, Choudhary RK, Sodroski J, Robinson JE. "Characterization of CD4-induced epitopes on the HIV type 1 gp120 envelope glycoprotein recognized by neutralizing human monoclonal antibodies". *AIDS Research and Human Retroviruses* 18(16):1207-1217 (2002).

Zhang W, Chipman PR, Corver J, Johnson PR, Zhang Y, Mukhopadhyay S, Baker TS, Strauss JH, Rossmann MG, Kuhn RJ. "Visualization of membrane protein domains by cryo-electron microscopy of dengue virus". *Nature Structural Biology* 10: 907-912 (2003).

List of Symbols, Abbreviations, and Acronyms

1.6D	anti-dengue virus human monoclonal antibody, neutralizing
2.3D	anti-dengue virus human monoclonal antibody, non-neutralizing
3.6D	anti-dengue virus human monoclonal antibody, non-neutralizing
3H5	anti-dengue virus mouse monoclonal antibody, recognizes E protein domain III
4.8A	anti-dengue virus human monoclonal antibody, neutralizing
4G2	anti-dengue virus mouse monoclonal antibody, recognizes E protein domain II
1OAN1	an E protein first domain I/domain II beta sheet connection region peptide
293T	human embryonic kidney cell line
aa	amino acid
Ab	antibody
ADE	antibody-dependent enhancement
ATCC	American Type Culture Collection
BSA	bovine serum albumin
bp	base pair
Br^{3}-	bromide anion
^{o}C	degree Celsius
C6/36	Asian tiger mosquito (*Aedes albopictus*) cell line
C=C	carbon double bond
(~C=C-C~)n	conjugated carbon double bonds
cDNA	complementary deoxyribonucleic acid
cm^{2}	square centimeters

CO_2	carbon dioxide
ConA	Concanavalin A
Cp	value used to estimate infectious units according to a standard curve
CTAC	cetyltrimethlammonium chloride
C-terminal	carboxyl terminal
C-terminus	carboxyl terminus
CryoEM	cryo electron microscopy
CTAB	cetyltrimethyl ammonium bromide
EDTA	ethylenediaminetetraacetic acid
D11C	anti-dengue virus human antibody, neutralizing
D11C.KL	anti-dengue virus human monoclonal antibody, neutralizing
DENV	dengue virus
DENV-1	dengue virus 1
DENV-1 HI-1	dengue virus 1 Hawaii strain 1
DENV-2	dengue virus 2
DENV-2 NG-C	dengue virus 2 New Guinea strain C
DENV-3	dengue virus 3
DENV-3 H-78	dengue virus 3 H strain 78
DENV-4	dengue virus 4
DENV-4 H-42	dengue virus 4 H strain 42
DMEM	Dulbecco's Modified Eagles' Medium
DMSO	dimethyl sulfoxide
DN57opt	an E protein domain II hinge region peptide
DN59	an E protein stem region peptide

DPX	p-xylene-bis-pyridinium bromide
E60	anti-dengue virus mouse monoclonal antibody, recognizes E protein domain II
ELISA	enzyme-linked immunosorbent assay
ENCAD	energy calculation and dynamics program
E protein	flavivirus envelope glycoprotein
FBS	fetal bovine serum
FFU	focus-forming units
h	hour
H_2O	water
H_2O_2	hydrogen peroxide
HEPES	4-(2-hydroxyethyl)-1-piperazineethanesulfonic acid
HIV-1	human immunodeficiency virus 1
HMAb	human monoclonal antibody
HRP	horseradish peroxidase
IC_{50}	fifty percent inhibitory concentration
IRB	Institutional Review Board
K-562	hematopoietic cells
K_D	dissociation constant
koff	dissociation rate constant
kon	association rate constant
L-amino acid	amino acid optical isomer, natural chirality
LLC-MK-2	rhesus monkey kidney epithelial cell line
M	dengue virus membrane protein

M	Molar
MEM	minimal essential medium
mg	milligram
min	minute
ml	milliliter
mM	millimolar
MMAb	mouse monoclonal antibody
MTT	3-(4,5-dimethylthiazol-2-yl)-2,5-diphenyltetrazolium bromide, a yellow tetrazole
NaBr	sodium bromide
NaOH	sodium hydroxide
Na_2SO_4	sodium sulfate
NH_3	ammonia
Ni^{+2}	nickel
NS1	dengue virus non structural protein 1
nm	nanometer
N-terminal	amino terminal
N-terminus	amino terminus
$\cdot O_2$-	superoxide
OD	optical density
OH-	hydroxide
$\cdot OH$	hydroxy radical
PBB	photobacterium broth
PBMC	peripheral blood mononuclear cells

PBS	phosphate buffered saline
PC	photocatalysis
PCR	polymerase chain reaction
pH	corresponds to concentration of hydronium ions in a solution
prM	dengue virus pre-membrane protein
qRT-PCR	quantitative real time PCR
RAPDF	residue-specific all-atom probability discriminatory function
retro-inverso	peptide with reversed amino acid sequence and D-amino acids
RFU	relative fluorescence units
RLU	relative light units
RNA	ribonucleic acid
ROR	radicals oxidants and reductants
rpm	revolutions per minute
RPMI-1640	Roswell Park Memorial Institute cell culture medium
s	second
S tag	streptavidin tag
SUV	small unilamellar vesicle
T7 phage	bacteriophage T7, a virus that infects bacteria
TECAN	a particular type of automatic well plate reader
THA	terephthalate
TiO_2	titanium oxide
TMB	3,3’,5,5’-tetramethylbenzidine
TTAC	tetradecyltrimethylammonium chloride
U	unit

μg	microgram
μl	microliter
μM	micromolar
UV	ultraviolet light
VIS	visible light
v/v	volume per volume
wt	wild type
w/v	weight per volume

DEPARTMENT OF DEFENSE

DEFENSE THREAT REDUCTION
AGENCY
8725 JOHN J. KINGMAN ROAD
STOP 6201
FORT BELVOIR, VA 22060
ATTN: H. MEEKS

DEFENSE TECHNICAL
INFORMATION CENTER
8725 JOHN J. KINGMAN ROAD,
SUITE 0944
FT. BELVOIR, VA 22060-6201
ATTN: DTIC/OCA

DEPARTMENT OF DEFENSE CONTRACTORS

QUANTERION SOLUTIONS, INC.
1680 TEXAS STREET, SE
KIRTLAND AFB, NM 87117-5669
ATTN: DTRIAC